Journal of New Media
DOI:10.32604/jnm.2021.024665
Article

Ground Nephogram Enhancement Algorithm Based on Improved Adaptive Fractional Differentiation

Xiaoying Chen[1,*], Jie Kang[1] and Cong Hu[2]

[1]College of Mechanical & Electrical Engineering, Sanjiang University, Nanjing, 210012, China

[2]Guangxi Key Laboratory of Automatic Detecting Technology and Instruments, Guilin University of Electronic Technology, Guilin, 541004, China

[*]Corresponding Author: Xiaoying Chen. Email: chenxiaoyingseu@163.com

Received: 16 September 2021; Accepted: 26 October 2021

Abstract: The texture of ground-based nephogram is abundant and multiplicity. Many cloud textures are not as clear as artificial textures. A nephogram enhancement algorithm based on Adaptive Fractional Differential is established to extract the natural texture of visible ground-based cloud image. Grunwald-Lentikov (G-L) and Grunwald-Lentikov (R-L) fractional differential operators are applied to the enhancement algorithm of ground-based nephogram. An operator mask based on adaptive differential order is designed. The corresponding mask template is used to process each pixel. The results show that this method can extract image texture and edge details and simplify the process of differential order selection.

Keywords: Ground nephogram; de-illumination; fractional differential; image enhancement

1 Introduction

The study of the identification for ground-based cloud type is very important to the automatic observation of ground nephoscope [1]. In order to reduce cloud image degradation caused by natural environment factors, such as light, rain, fog and dust and so on, the cloud image should be preprocessed before recognition to extract the useful information of the ground-based cloud as much as possible [2]. Image classification is an important part in domain-specific application image mining [3]. There exist many problems such as loud noises, unclear images of optical imaging instruments for obtaining ground-based clouds in the research of automatic recognition of ground clouds. It is hard to get precise identification of cloud image for user because of the impact of natural environment factors, such as light, rain, fog and dust and so on [4–5]. Therefore, the cloud image should be preprocessed while extracting the useful information of the ground-based cloud as much as possible. Differential tools are used in many image enhancement pre-processing studies [6].

Fractional calculus is not only an important branch of mathematical analysis, but also one of the mathematical foundations for fractal theory. The application of fractional calculus to image signal processing can extract complex texture details from two-dimensional image signals by its sensitivity to image details. In this way, the edge of the image is obviously enhanced and the texture details of the image are clearer.

Research shows that when the differential order $\gamma \geq 1$, the higher the differential order is, the weaker the low frequency part will be, while enhancing the high frequency part of the signal. When $0 < \gamma < 1$, the non-linear preservation of information can properly enhance the high and medium frequency part of the signal without weakening the very low frequency part of the signal. Therefore, the application of fractional differentiation not only preserve the low-frequency contour feature of a digital image as far as

possible, but also enhance the high-frequency texture feature with a relatively large gray jump in digital image [7].

The texture of ground-based cloud images is abundant and multiplicity. It is difficult to extract features of ground-based cloud images because they are not as clear as artificial textures. In this paper, the fractional differential method is used to enhance the cloud images which are helpful to further extract the texture features of cloud images.

2 Extraction of Image Texture by Fractional Differential

So far, there is no unified standard definition of fractional differential. The common definitions are R-L, G-L, Cauchy and Caputo [8]. Among them, R-L, Cauch and Caputo definitions have high computational complexities which go against the calculation of very large datasets. While G-L definitions are more accurate in practical applications and are very suitable for applications in signal processing field [9].

2.1 G-L Definition

Fractional differential G-L [10] definition equation is derived by extending the order of calculus from integer to fraction according to the definition of integer derivative. The γ order G-L fractional differential of the signal $f(t) \in [a,t](a < t, a \in R, t \in R)$ is constructed using

$$ {}_{a}^{G}D_{t}^{\gamma} f(t) = \lim_{h \to 0} \frac{1}{h^{\gamma}} \sum_{m=0}^{\frac{t-a}{h}} (-1)^{m} \frac{\Gamma(\gamma+1)}{m!\Gamma(\gamma-m+1)} f(t-hm) \tag{1} $$

where Gamma Function is $\Gamma(n) = \int_0^{\infty} e^{-t} t^{n-1} \mathrm{d}t = (n-1)!$.

Duration of signal $f(t)$ is $t \in [a,t]$. If $[a,t]$ is by equal division method according to the interval of $h = 1$ then $n = [\frac{t-a}{h}] = [t-a]$. The differential form of fractional differential of one-dimensional signal can be obtained using

$$ \begin{aligned} \frac{d^{\gamma} f(t)}{dt^{\gamma}} \approx\ & f(t) + (-\gamma) f(t-1) + \frac{(-\gamma)(-\gamma+1)}{2} f(t-2) + \\ & \cdots + \frac{\Gamma(-\gamma+1)}{n!\Gamma(-\gamma+n+1)} f(t-n) \end{aligned} \tag{2} $$

Generally, on an image f of $M \times N$ pixel, linear filtering can be obtained by a filter mask of $m \times n$ size [11]:

$$ g(x,y) = \sum_{s=-a}^{a} \sum_{t=-b}^{b} w(s,t) f(x+s, y+t) \tag{3} $$

where $w(s,t)$ denotes the mask operator of filtering mask point (s,t). $f(x,y)$ is the gray value of image with point (x,y). $a = (m-1)/2$ and $b = (n-1)/2$. All the pixels in the image for $x = 0,1,2,\cdots,M-1$ and $y = 0,1,2,\cdots,N-1$ must be filtered using Eq. (3). The 5 × 5 fractional differential mask is selected to construct an isotropic filter. The masking operator Tiansi [12] is obtained, as in Fig. 1.

The image edge information can be extracted from the Tiansi operator, as in Fig. 1. Firstly, the Tiansi masking operator is normalized. Then the image is operated with the convolution calculation using Tiansi template. In this way, not only the low-frequency component of the original image can be retained, but also the high-frequency component of the original image can be greatly enhanced. After that, the image filtered by Tiansi mask is subtracted from the original image and the edge information of the image can be obtained.

$\frac{\gamma^2-\gamma}{2}$	0	$\frac{\gamma^2-\gamma}{2}$	0	$\frac{\gamma^2-\gamma}{2}$
0	-γ	-γ	-γ	0
$\frac{\gamma^2-\gamma}{2}$	-γ	8	-γ	$\frac{\gamma^2-\gamma}{2}$
0	-γ	-γ	-γ	0
$\frac{\gamma^2-\gamma}{2}$	0	$\frac{\gamma^2-\gamma}{2}$	0	$\frac{\gamma^2-\gamma}{2}$

Figure 1: Tiansi fractional differential operator masking

2.2 R -L Definition

R-L [13] definition method is seldom used in image processing field. The fractional integration of signal R-L with γ order can be obtained using

$$ {}_a^R D_t^\gamma f(t) = \frac{d^\gamma f(t)}{[d(t-a)]^\gamma} = \frac{1}{\Gamma(-\gamma)} \int_a^t (t-\xi)^{-\gamma-1} f(\xi) d\xi \quad , \gamma < 0 \tag{4} $$

where ${}_a^R D_t^\gamma$ denotes fractional integral operator based on R-L definition, R is a real number set, t and a are the range of integration. For any positive integer n and real number γ fractional integral of the signal $f(t)$ becomes

$$ {}_a^R D_t^\gamma f(t) = \frac{d^n}{dt^n} \frac{d^{\gamma-n} f(t)}{[d(t-a)]^{\gamma-n}} = \frac{d^n}{dt^n} [{}_a^R D_t^{\gamma-n} f(t)] \tag{5} $$

The γ order R-L fractional differential of the signal $f(t)$ is computed from Eq. (4) and Eq. (5) as follows:

$$ {}_a^R D_t^\gamma f(t) = \sum_{k=0}^{n-1} \frac{(t-a)^{k-\gamma} f^{(k)}(a)}{\Gamma(k-\gamma+1)} + \frac{1}{\Gamma(n-\gamma)} \int_a^t \frac{f^{(n)}(\xi)}{(t-\xi)^{\gamma-n+1}} d\xi \quad , 0 \le \gamma < n \tag{6} $$

where $\frac{d^n}{dt^n}$ is an integral order differentiation, n is the smallest integer to meet $\gamma - n < 0$. When $a = 0, n = 1$, ${}_a^R D_t^\gamma f(t)$ is constructed using

$$ \begin{aligned} {}_a^R D_t^\gamma f(t) &= \frac{t^{-\gamma} f(0)}{\Gamma(1-\gamma)} + \frac{1}{\Gamma(1-\gamma)} \int_0^t \frac{f^{(1)}(\xi)}{(t-\xi)^\gamma} d\xi \\ &\cong \frac{1}{\Gamma(1-\gamma)} \left[\frac{f(0)}{t^\gamma} + \sum_{k=0}^{N-1} \int_{kt/N}^{(kt+t)/N} \left(\frac{d}{d\xi} f(t-\xi) \frac{d\xi}{\xi^\gamma} \right) \right] \end{aligned} \quad , 0 \le \gamma < 1 \tag{7} $$

Without losing generality, let $a = 0$. The duration $[0,t]$ of signal $f(t)$ is divided into N equal division. Then $N+1$ total of nodes are obtained. Each node can be obtained using $F_N = f(0)$, $F_{N-1} = f(t/N), \cdots, F_k = f(t - kt/N), \cdots, F_0 = f(t)$.

$\int_{kt/N}^{(kt+t)/N} \left(\frac{d}{d\xi} f(t-\xi) \frac{d\xi}{\xi^\gamma} \right)$ is computed from the difference approximation formula of the first derivative as follows:

$$\int_{kt/N}^{(kt+t)/N}\left(\frac{d}{d\xi}f(t-\xi)\frac{d\xi}{\xi^{\gamma}}\right)\cong\frac{f\left(t-\frac{kt}{N}\right)-f\left(t-\frac{t}{N}-\frac{kt}{N}\right)}{t/N}\int_{kt/N}^{(kt+t)/N}\frac{d\xi}{\xi^{\gamma}} \tag{8}$$
$$=\frac{t^{-\gamma}N^{\gamma}}{1-\gamma}(f_k-f_{k+1})[(k+1)^{1-\gamma}-k^{1-\gamma}]$$

Substituting Eq. (8) into Eq. (7), it will generate Eq. (9) as follows:

$$\frac{d^{\gamma}}{dt^{\gamma}}f(t)=\frac{t^{-\gamma}N^{\gamma}}{\Gamma(2-\gamma)}\frac{(1-\gamma)f_N}{N^{\gamma}}+ \tag{9}$$
$$\frac{t^{-\gamma}N^{\gamma}}{\Gamma(2-\gamma)}\left\{\sum_{k=0}^{N-1}(f_k-f_{k+1})[(k+1)^{1-\gamma}-k^{1-\gamma}]\right\}\quad,0\le\gamma<1$$

where minimum equidistant interval is $h=1$. When $k=n\le N-1$, the post-term difference formula of fractional partial differential of two-dimensional image $f(x,y)$ in the negative direction of X and Y axes (expressed by W_{x-} and W_{y-}, respectively) can be derived from Eq. (9).

Linear filtering is performed using filter mask of $m\times n$ size for image f. The masking coefficient with order ($0<\gamma<1$) of R-L fractional differential operator is computed from Eq. (9) as follows [14]:

$$\begin{cases} C_0=\dfrac{1}{\Gamma(2-\gamma)} \\ C_1=\dfrac{2^{1-\gamma}-2}{\Gamma(2-\gamma)} \\ \vdots \\ C_k=\dfrac{(k+1)^{1-\gamma}-2k^{1-\gamma}+(k-1)^{1-\gamma}}{\Gamma(2-\gamma)} \\ \vdots \\ C_{n-1}=\dfrac{n^{1-\gamma}-2(n-1)^{1-\gamma}+(n-2)^{1-\gamma}}{\Gamma(2-\gamma)} \\ C_n=\dfrac{(1-\gamma)n^{-\gamma}-n^{1-\gamma}+(n-1)^{1-\gamma}}{\Gamma(2-\gamma)} \end{cases} \tag{10}$$

The Riemann-Liouville fractional-order differential template with 5 × 5 isotropy is constructed as in Fig. 2.

C_2	0	C_2	0	C_2
0	C_1	C_1	C_1	0
C_2	C_1	$8C_0$	C_1	C_2
0	C_1	C_1	C_1	0
C_2	0	C_2	0	C_2

Figure 2: Isomorphic R-L fractional differential operator mask with 5 × 5

Similarly, the above masks are normalized through each item dividing by the sum of the masking coefficients, i.e., $(8C_0+8C_1+8C_2)$. Then the mask is used to convolute computation for the image. The image and operator template are moved point by point to realize fractional differential filtering in spatial domain. Compared G-L definition with R-L definition has the same structure, but the differential coefficients of corresponding positions are different. Similarly, the image edge can be extracted by fractional differential operation by subtracting the original image from the filtered image.

3 Cloud Enhancement Algorithm Based on Adaptive Fractional Differential

The Gauss difference receptive field symmetry model of fractional differential for the image [15] shows that the enhancement of texture details in regions with gentle gray change is more obvious by fractional differential. Traditional fractional differential has incomparable advantages in describing fractal dimension space. Therefore, using fractional differential to process the complex texture information of digital image [16] can enhance nonlinearly the high frequency component and retain the middle and low frequency texture information [17]. However, different window sizes and multi-scale fractional differential masks need to be designed to process images in order to get the best image enhancement effect. Finding the best fractional differential order manually will greatly increase the computing time. It is not conducive to real-time processing of a large number of images. A method of automatically generating fractional differential order is proposed [18] to realize automatically according to the theory of mask window, definition formula of fractional differential, gradient characteristics of the image and human visual characteristics.

The essence of digital image processing by fractional differential is that different frequency parts of the image are processed nonlinearly. Therefore, starting from the characteristics of different frequency parts of the image and processing using by different fractional differential orders at different frequencies that can realize the adaptive fractional differential definite order.

In this paper, a feature of the gradient direction for an image is described. The gradient direction reflects the magnitude and direction of the maximum gray change at each pixel of the image [19]. The ability of human eyes to distinguish gray level is very poor when the gray level is very high or very low [20]. For example, in the vicinity of 0 gray level, only 8 gray levels can be distinguished, and in the vicinity of 255 gray levels, 3 gray levels can be distinguished. When the gray level is moderate, the human eye has the strongest ability to distinguish the gray level. If the gray level is about 128, the human eye can distinguish two gray levels.

The gradient of an image at its pixels (x, y) is defined as $G[f(x, y)]$ and its modulus can be obtained:

$$mag(G[f(x,y)]) = \sqrt{G'^2_x + G'^2_y} = [(\frac{\partial f}{\partial x})^2 + (\frac{\partial f}{\partial y})^2] \tag{11}$$

The speed of gray level change in spatial domain reflects the gradient of image. The human eye will pay more attention to the region with large gray level change than to the region with slow gray level change. The gray value of pixels whose gradient modulus is less than 2 remains unchanged. For the pixels whose gradient modulus is between 2 and 90 (the gray-level change is small) this area is rich in texture details but not easy to attract attention of the human eye. Therefore, the gray-level interval should be strengthened appropriately. For pixels whose gradient modulus is greater than 90 (edge contour region of image with sharp gray change), the gray interval should be restricted appropriately [21].

So the functions of fractional differential order γ and $mag(G)$ can be obtained:

$$\gamma = \begin{cases} \dfrac{1}{\max'(G) + \varepsilon_1} \cdot mag(G) + \{\varepsilon_2\}, & mag(G) > 90 \\ 0 \qquad\qquad\qquad\qquad\quad , & mag(G) \le 2 \end{cases} \tag{12}$$

where $\max'(G)$ is the maximum of the gradient modulus, ε_1 is an arbitrary positive number, and a set positive parameter ε_2 is added. It can highlight the effect of mask center point on neighborhood points to satisfy the following formula:

$$\varepsilon_2 < 1 - \frac{1}{\max'(G) + \varepsilon_1} \cdot mag(G) \tag{13}$$

When $mag(G) > 90$, use $\varepsilon_1 = \max'(G)$. So $\varepsilon_2 < 0.5$, $\varepsilon_2 = 0.499$. When $2 < mag(G) \le 90$, we intend to use $\varepsilon_1 = 2\max'(G)$. So $\varepsilon_2 < 0.666$, $\varepsilon_2 = 0.666$. Thus, the functions of differential order γ and $mag(G)$ can be obtained as follows:

$$\gamma = \begin{cases} \dfrac{1}{2\max'(G)} \cdot mag(G) + 0.499 & ,90 < mag(G) \\ \dfrac{1}{3\max'(G)} \cdot mag(G) + 0.666 & ,2 < mag(G) \le 90 \\ 0 & ,mag(G) \le 2 \end{cases} \tag{14}$$

According to the above formula, when $mag(G)$ is large, the gray value of the image representing its edge contour changes greatly. The fractional differential order γ decreases appropriately. When $mag(G)$ is small, the region texture is dense and the gray level changes slightly. The fractional differential order γ increases appropriately. If the fractional differential order is zero, it means the equal gray level area or the gentle change area which does not need to be processed. Only the corresponding gray level of the image is preserved.

4 Texture Extraction Results and Quantitative Contrast Experiments

In order to verify the effectiveness of fractional differential method in extracting the texture of ground-based cloud images, experiments were carried out on several groups of cloud images. In addition to the intuitive qualitative verification, the quantitative research is also carried out according to the extraction results. Firstly, the ten types cloud images are captured with 512 × 512 pixels, and then the features of cloud images are extracted by fractional differential method.

The first method is to define fractional differential G-L of order manually. Four typical orders, $\gamma = 0.3$, $\gamma = 0.55$, $\gamma = 0.7$ and $\gamma = 0.9$ are used, respectively. The texture images of 10 types different cloud samples are processed by adaptive γ order differential and several specified order fractional differential methods respectively, and the texture enhancement ability of cloud images is compared. The experimental results are given in Fig. 3. Figs. 3 a0–j0 is a cloud sample of ten types. Among them, there are not only cumulus humilis and cumulonimbus with clear outline texture, but also cirrus and cirrostratus with abundant detailed texture, and stratus, and nimbostratus with less obvious texture. The orders of Fractional Differential processed clouds (Figs. 3a2–j2) are 0.3. The orders are 0.55 in Figs. a3–j3. The orders are 0.7 in Figs. 3a4–j4. Orders are 0.9 in Figs. 3a5–j5. From the processing results of ten types cloud images, the fractional differential extraction of cloud images with abundant texture information is effective. However, the effect of cloud images with less obvious texture is not good. The results of 0.3-order fractional derivative extraction for some clouds with abundant texture are as in Figs. 3a2, b2, g2, i2, j2. The details and textures of cloud images can be extracted but the enhancement effect is too weak and the extraction effect is not obvious. With the increase of differential order between 0 and 1 the image enhancement becomes larger and the texture becomes clearer, but the detail texture is lost. When dealing with texture images, the texture details can be extracted adaptively in Figs. 3a1–j1. It has good texture extraction effect, but it is not as good as the best treatment effect of 0.9 order.

Then R-L is defined by using $\gamma = 0.3$, $\gamma = 0.55$, $\gamma = 0.7$ and $\gamma = 0.9$ as the specified fractional differential order, respectively. At the same time, the fractional differential order adaptive algorithm proposed is used. A comparative experiment of ten types cloud images is carried out on the above different cloud images and the results are shown in Fig. 4. Fig. 4 shows under R-L definition, the results of adaptive selection of differential order also retain the texture details of the original image, but it is also not as good as the best processing effect of 0.9 order.

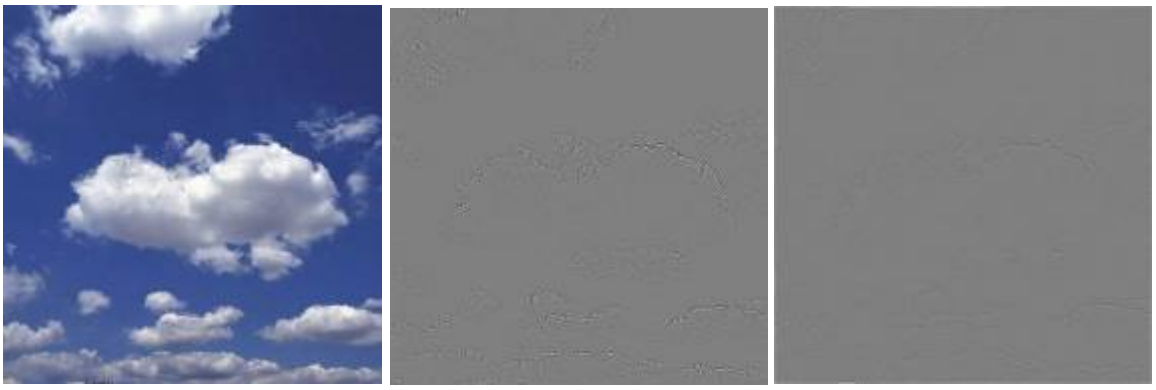

(a0) (a1) (a2)

(a3) (a4) (a5)

(b0) (b1) (b2)

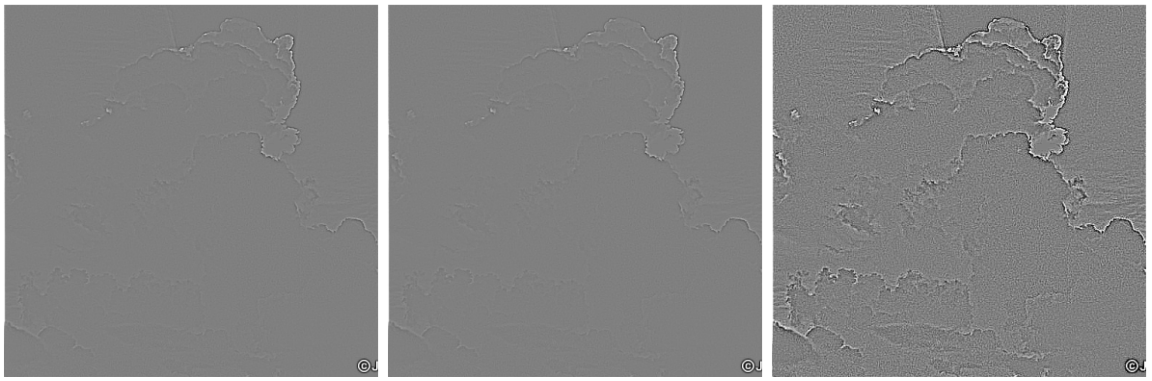

(b3) (b4) (b5)

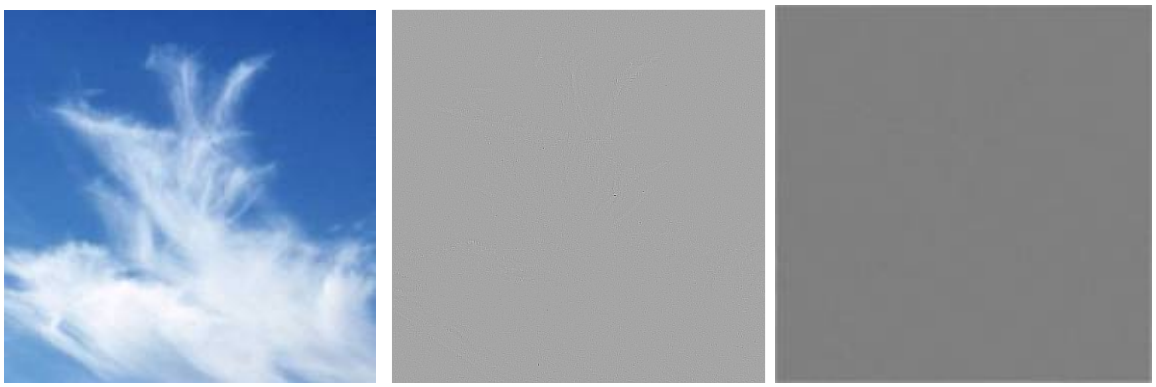

(c0) (c1) (c2)

(c3) (c4) (c5)

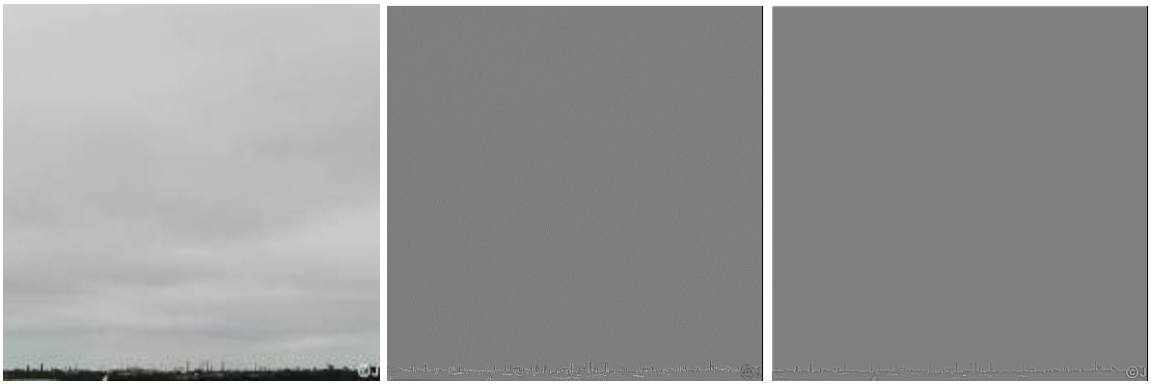

(d0) (d1) (d2)

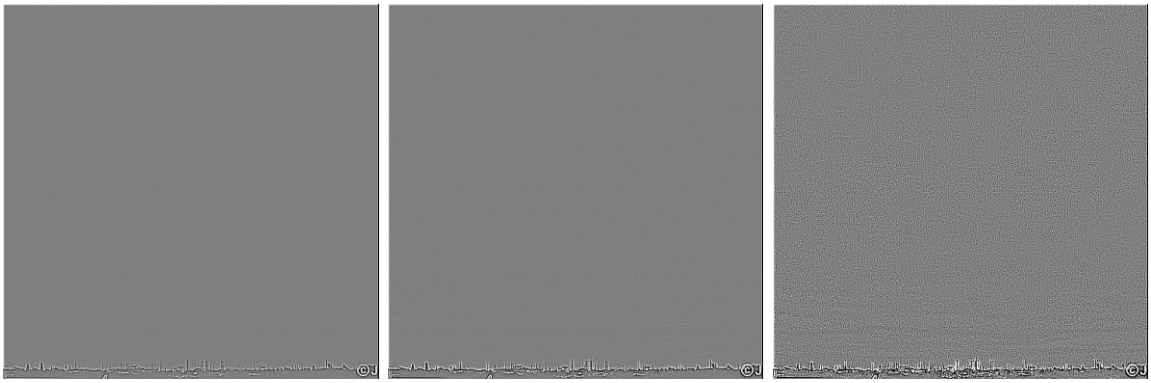

(d3) (d4) (d5)

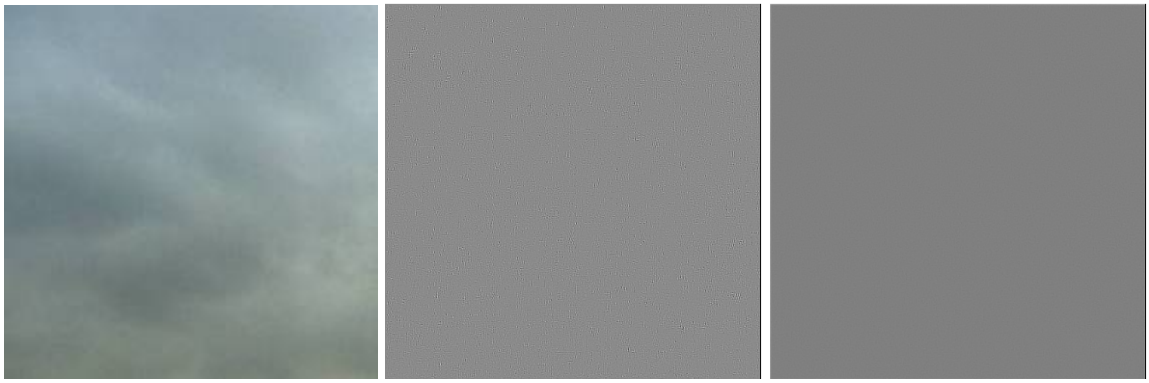

(e0) (e1) (e2)

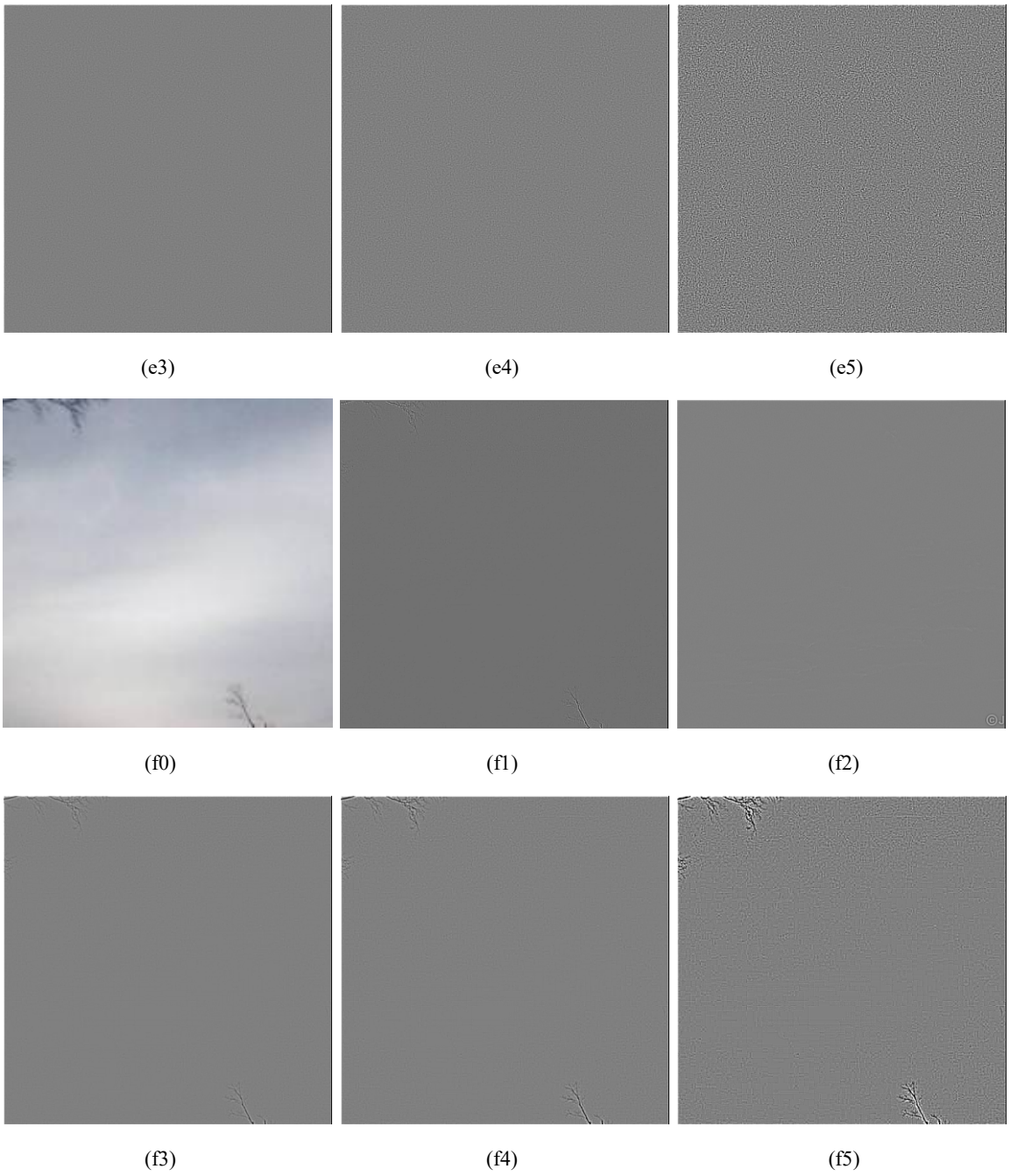

(e3) (e4) (e5)

(f0) (f1) (f2)

(f3) (f4) (f5)

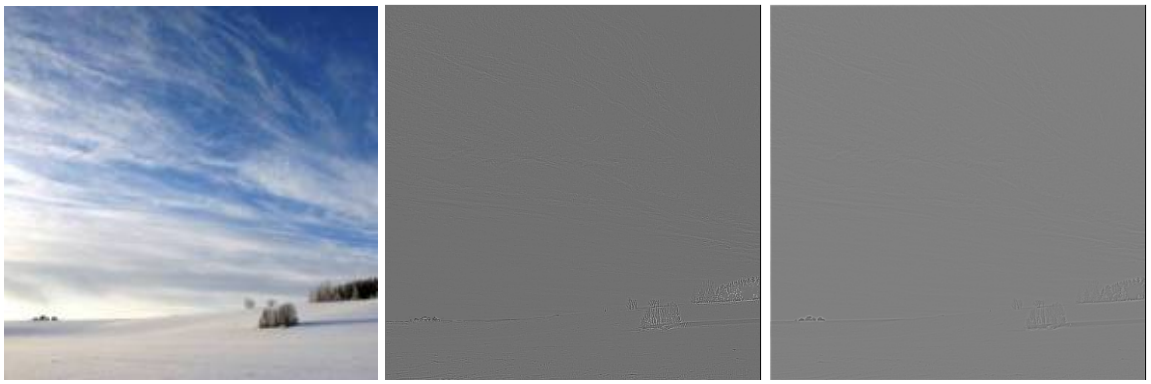

(g0) (g1) (g2)

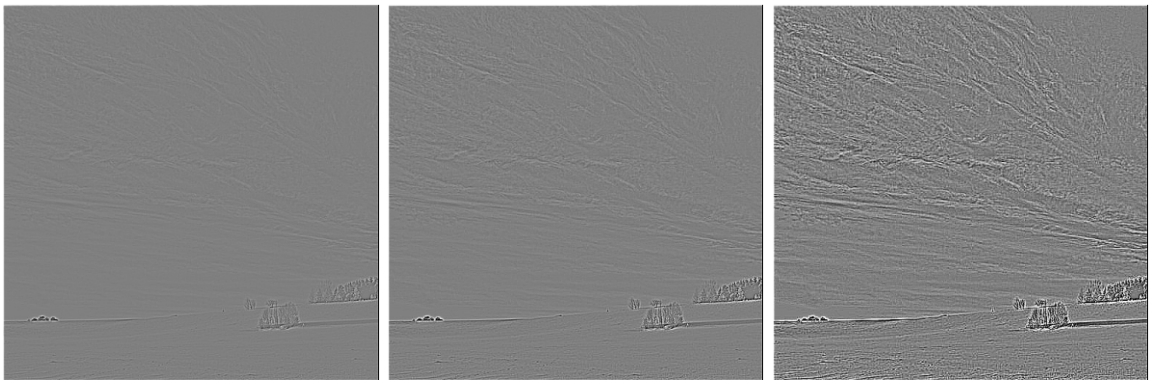

(g3) (g4) (g5)

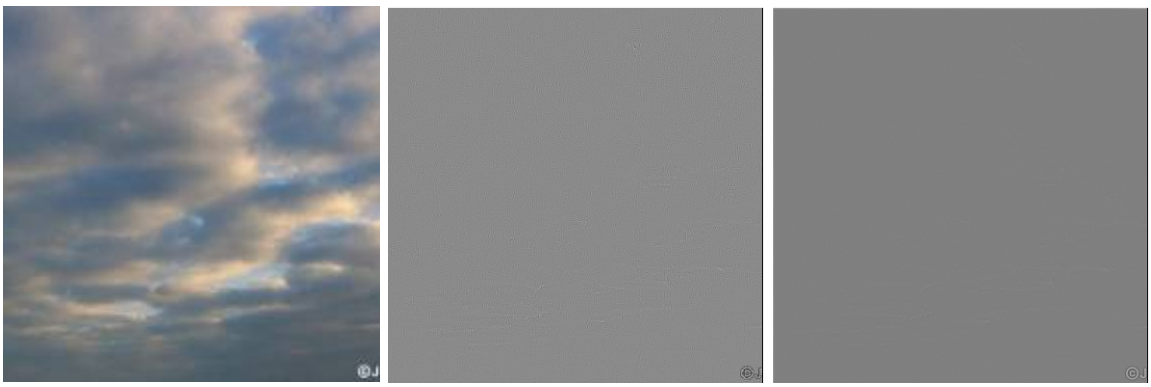

(h0) (h1) (h2)

(h3) (h4) (h5)

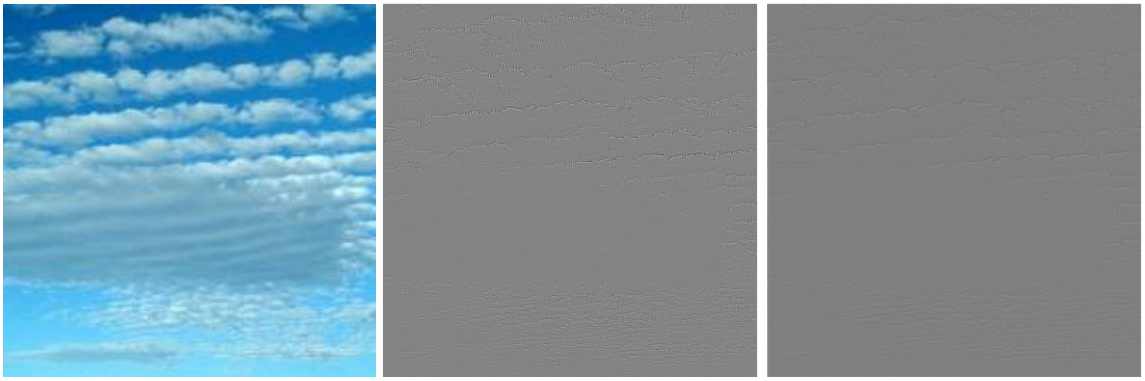

(i0) (i1) (i2)

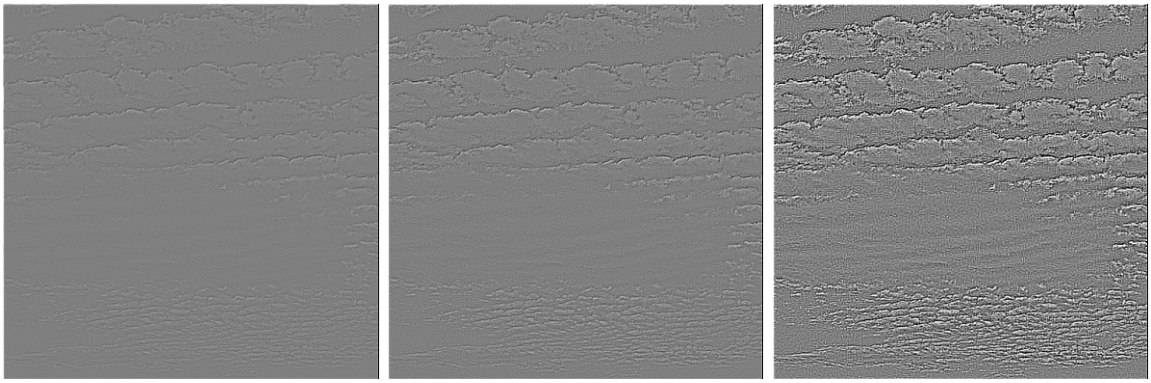

(i3) (i4) (i5)

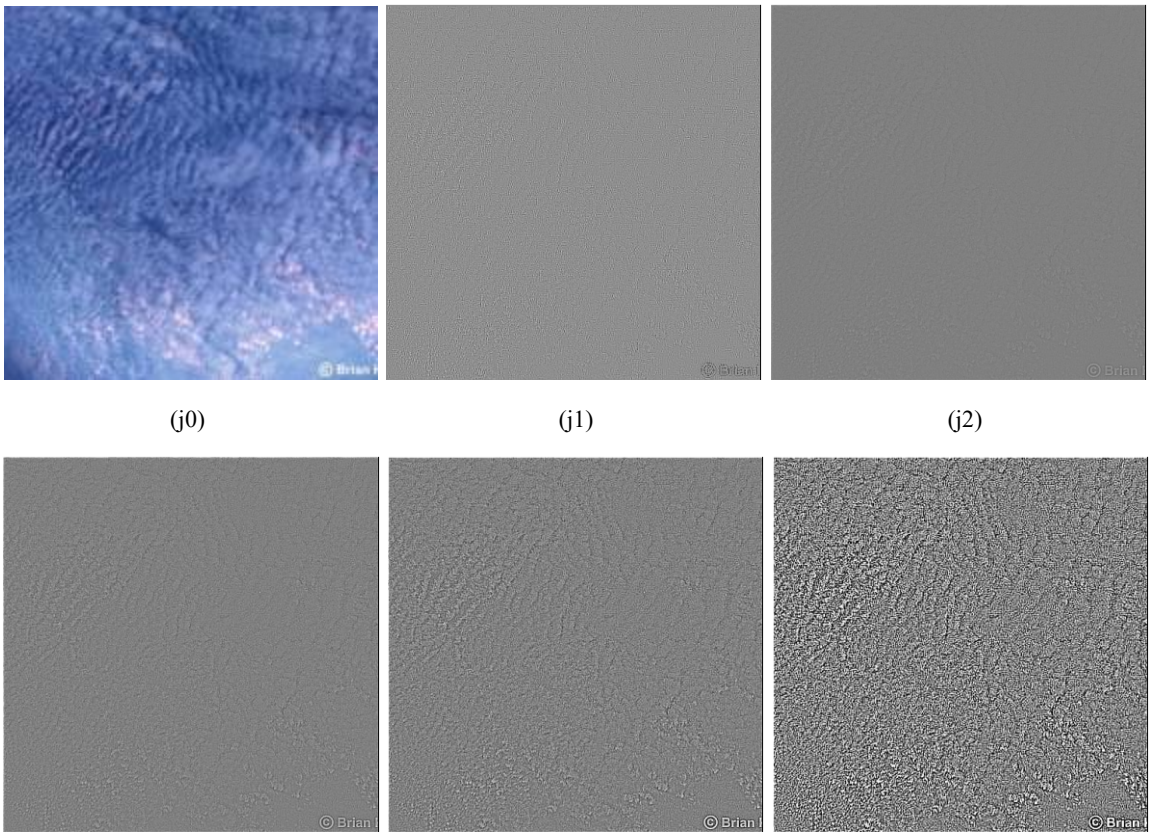

(j0) (j1) (j2)

(j3) (j4) (j5)

Figure 3: G-L definition extraction results: (a0)–(j0) Cumulus Humilis 3, Cumulonimbus 1, Cirrus 1, Stratus 1, Nimbostratus 5, Altostratus 5, Stratocirrus 3, Stratocumulus 2, Altocumulus 7 and Cirrocumulus 1; (a1)–(j1) is an adaptive fractional differential; (a2)–(j2) is of order 0.3; (a3)–(j3) is of order 0.55; (a4)–(j4) is of order 0.7; (a5)–(j5) is of order 0.9

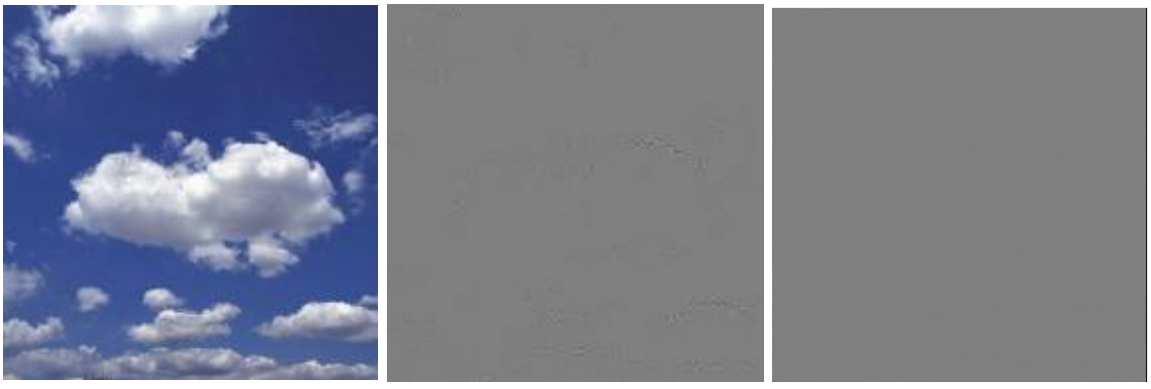

(a0) (a1) (a2)

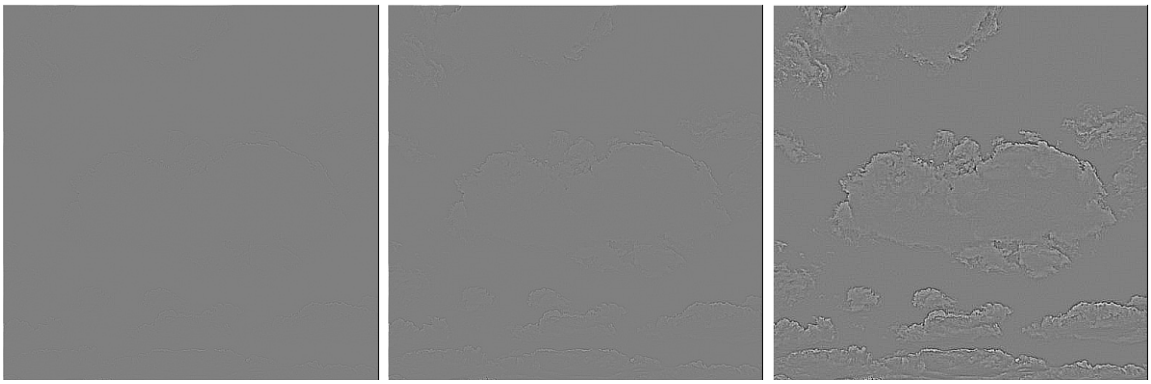

(a3) (a4) (a5)

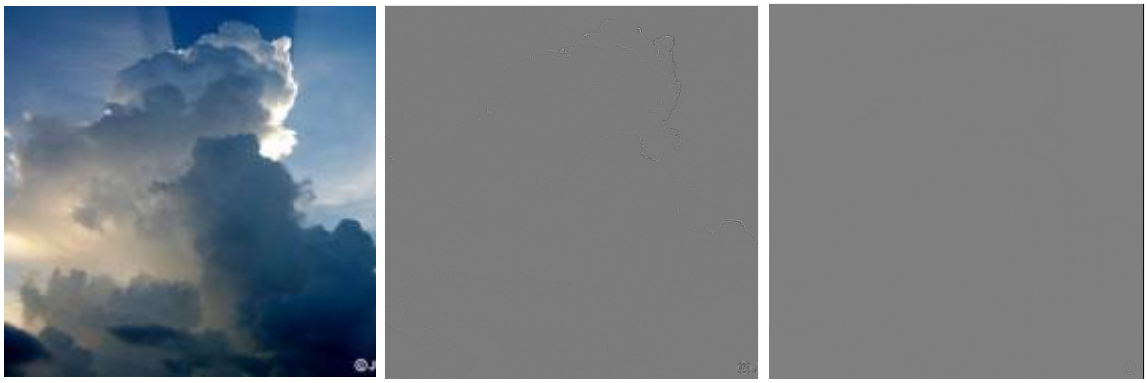

(b0) (b1) (b2)

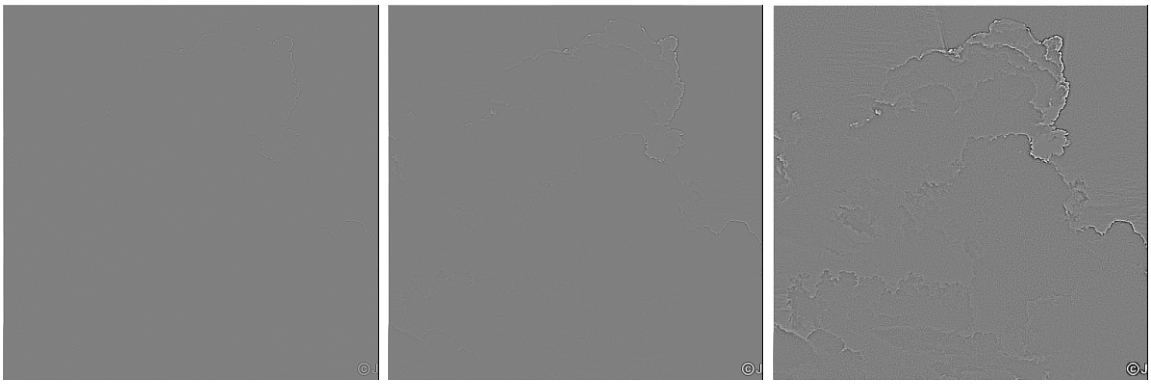

(b3) (b4) (b5)

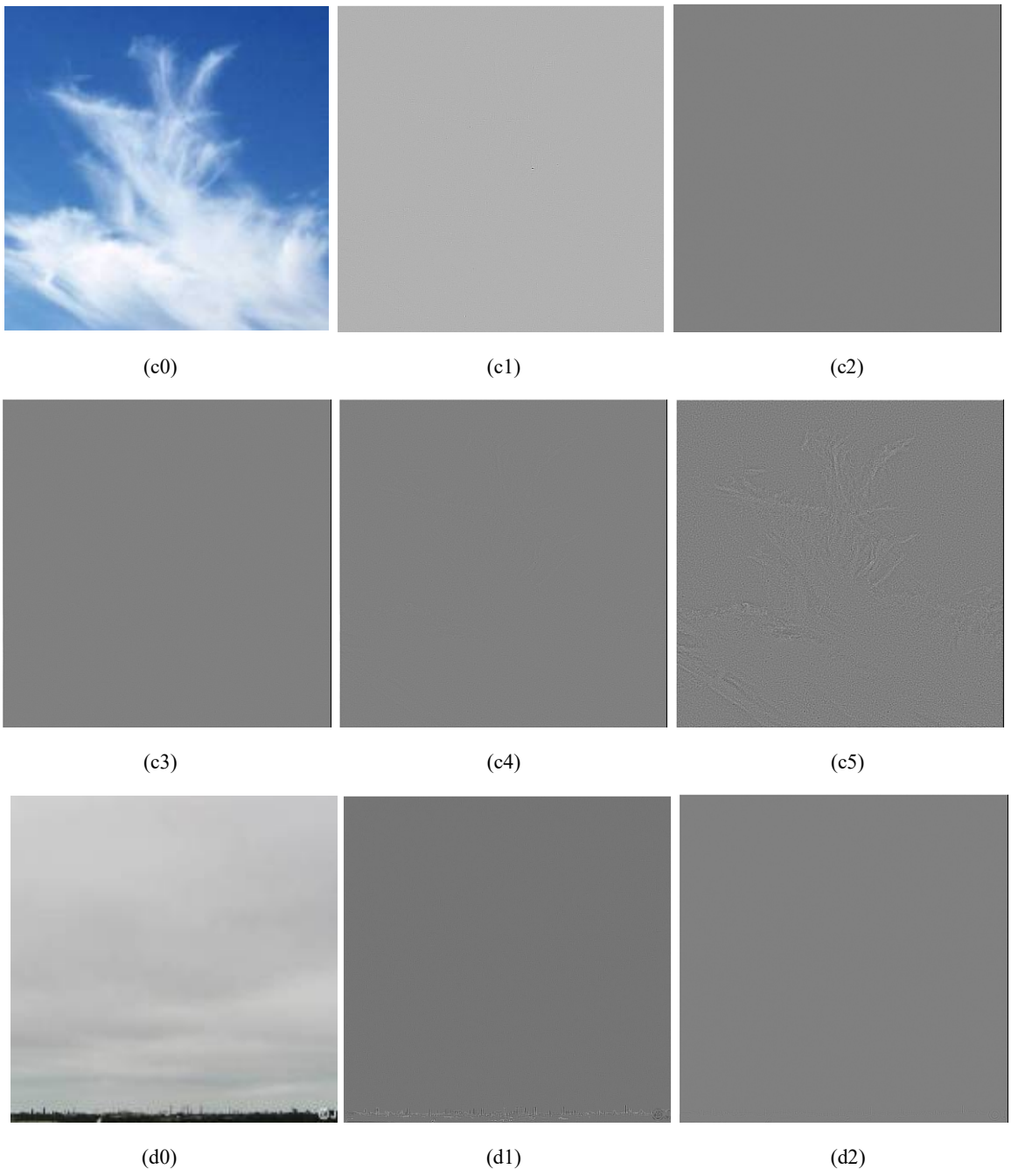

(c0) (c1) (c2)

(c3) (c4) (c5)

(d0) (d1) (d2)

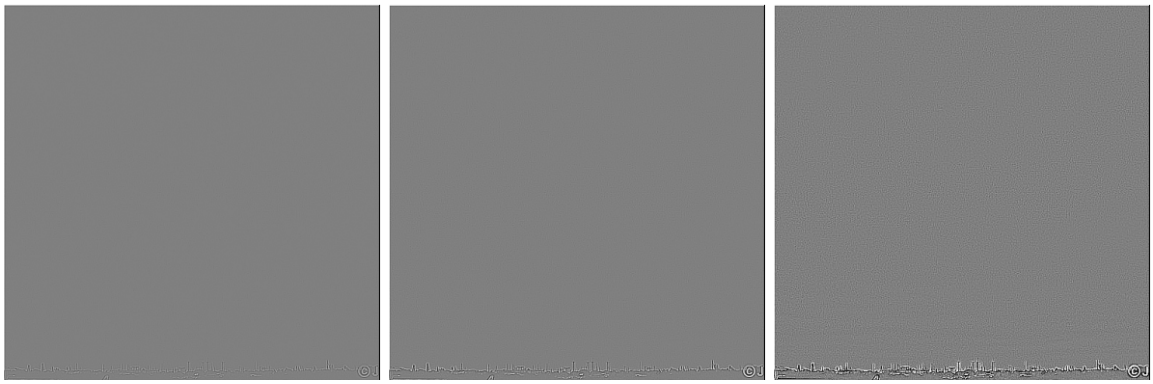

(d3) (d4) (d5)

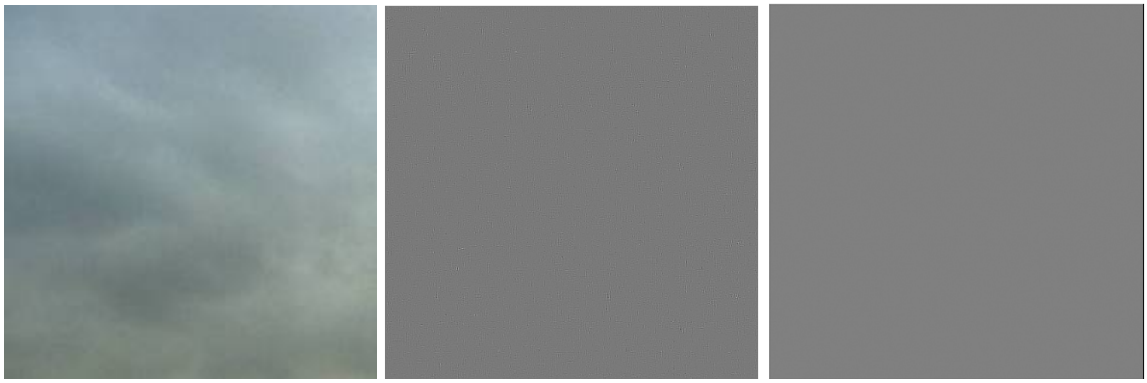

(e0) (e1) (e2)

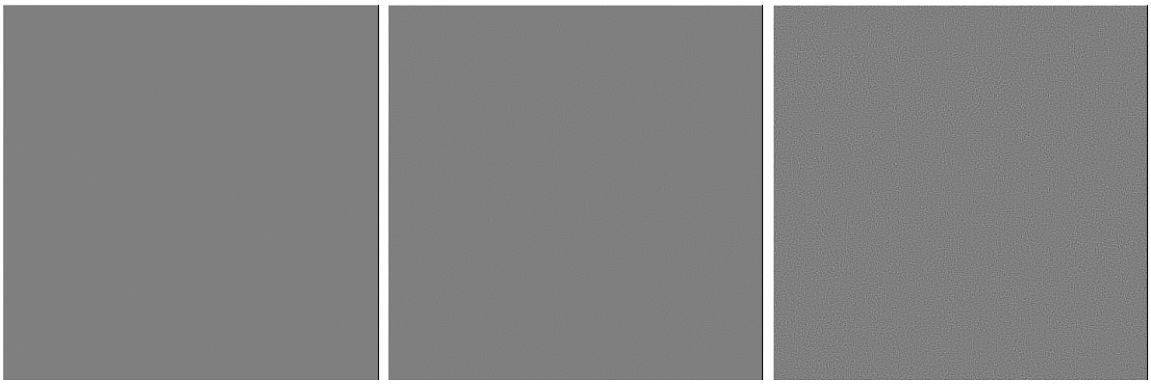

(e3) (e4) (e5)

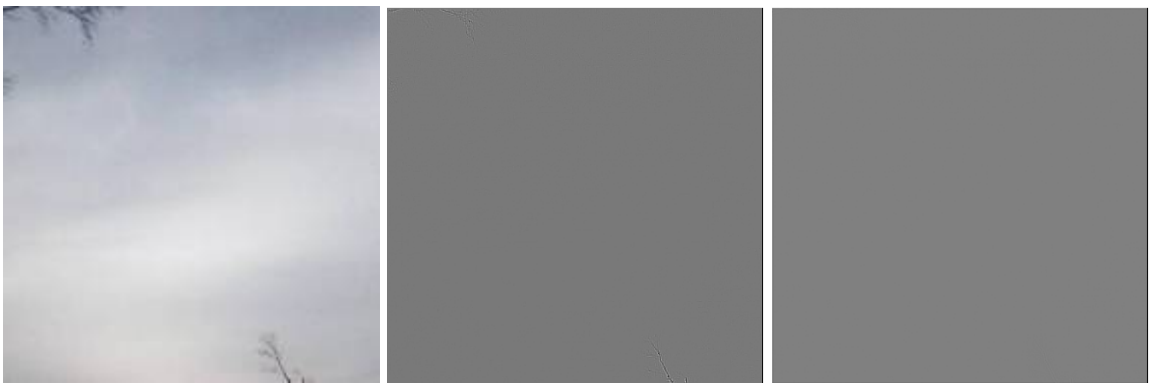

(f0) (f1) (f2)

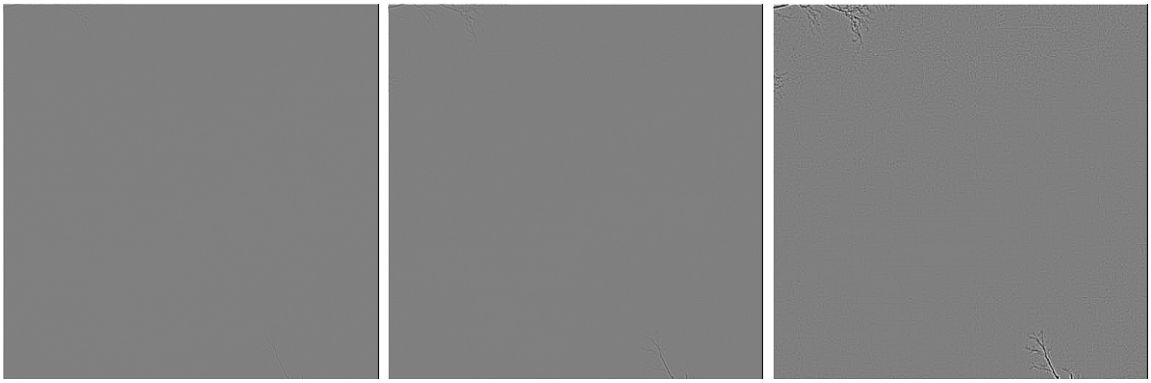

(f3) (f4) (f5)

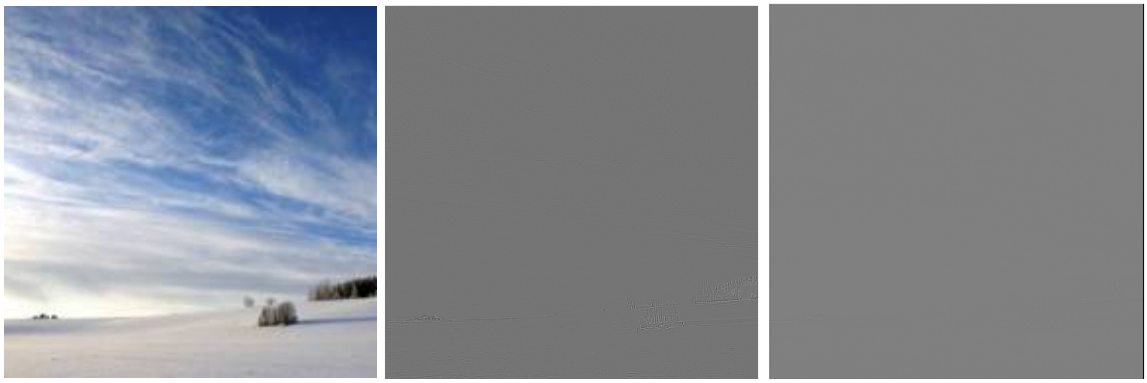

(g0) (g1) (g2)

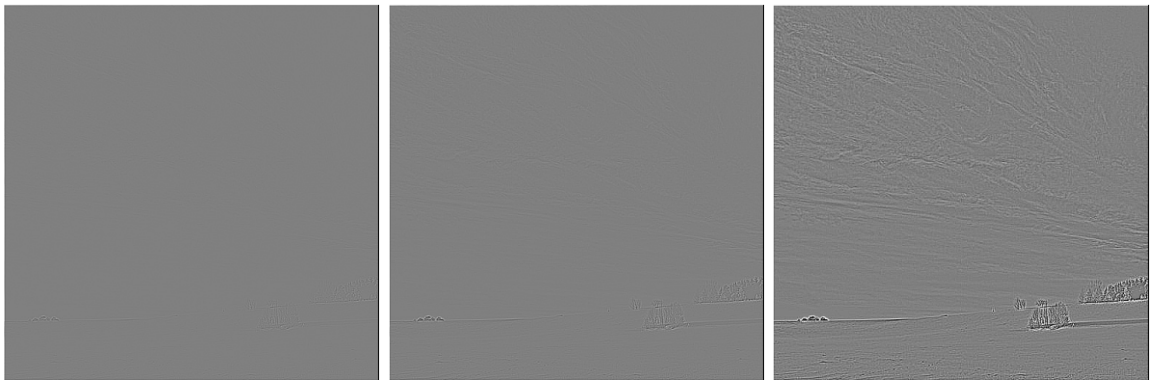

(g3) (g4) (g5)

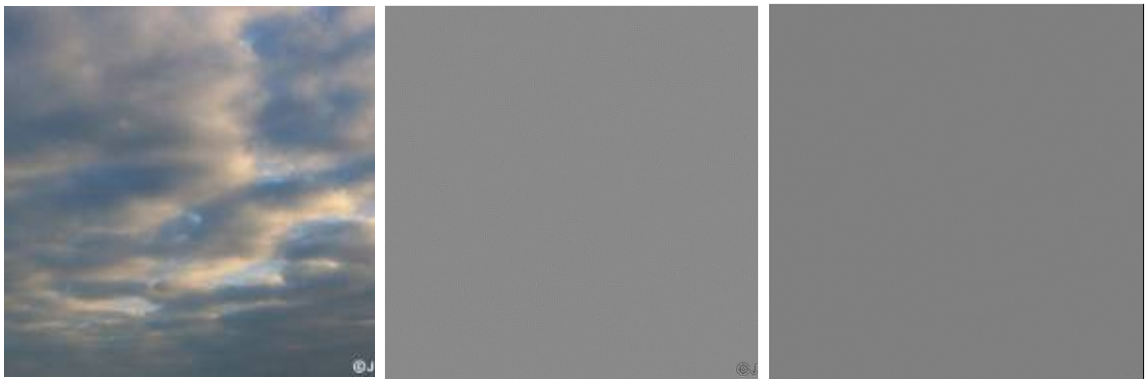

(h0) (h1) (h2)

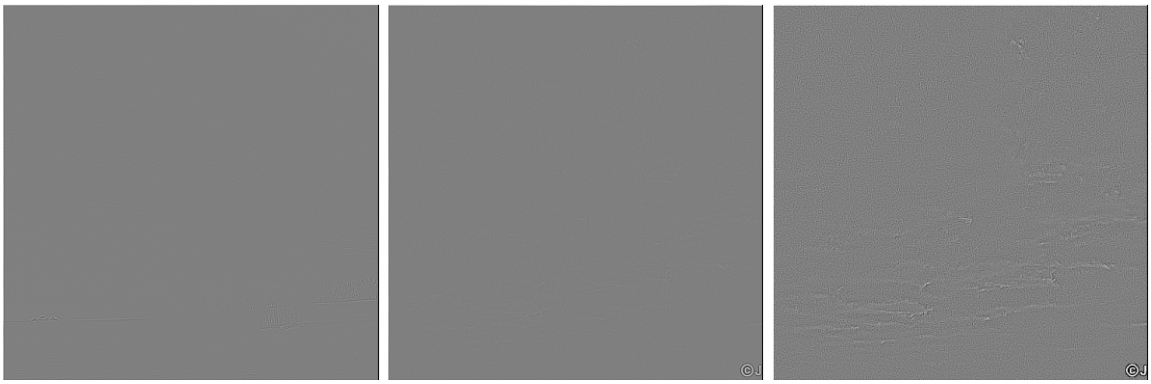

(h3) (h4) (h5)

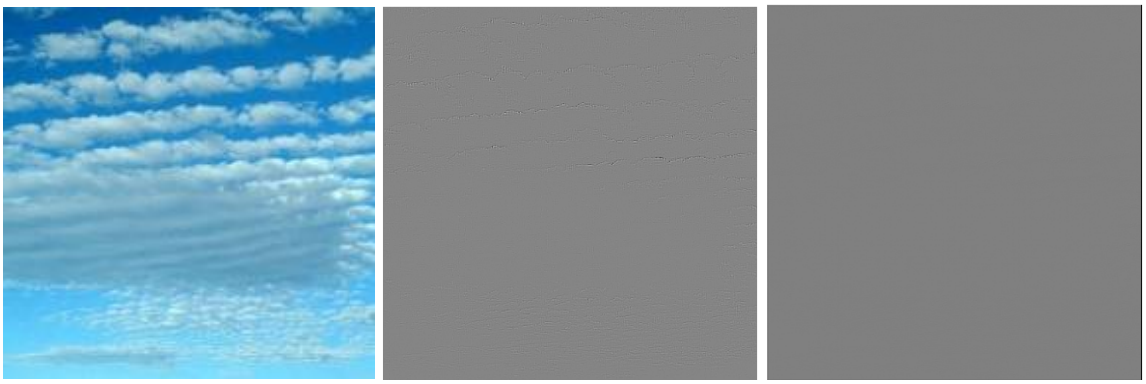

(i0) (i1) (i2)

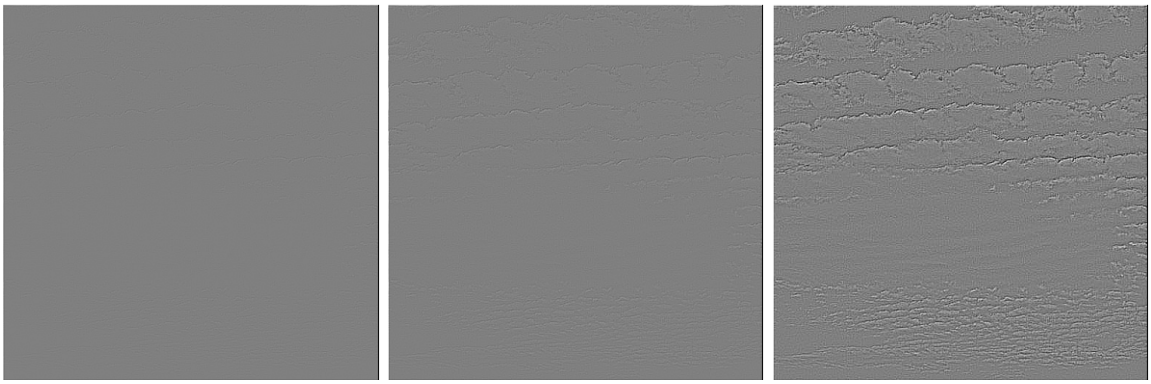

(i3) (i4) (i5)

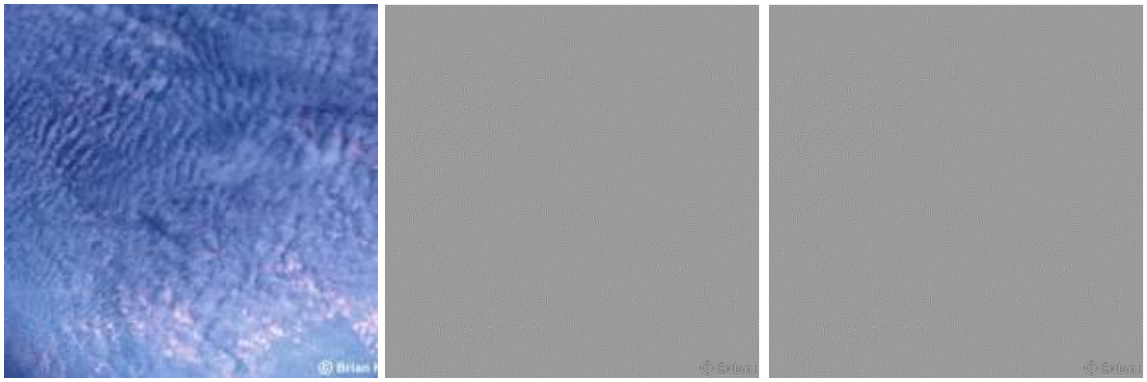

(j0) (j1) (j2)

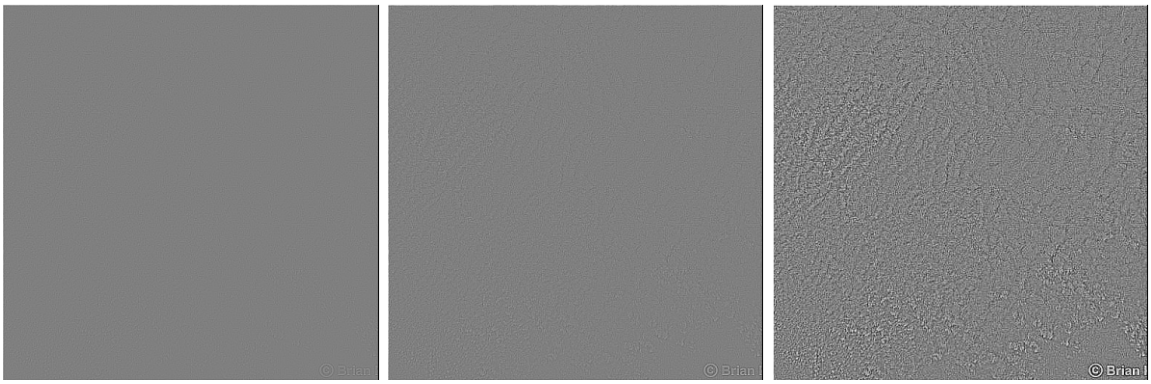

(j3) (j4) (j5)

Figure 4: R-L definition extraction results: (a0)–(j0) Cumulus Humilis 3, Cumulonimbus 1, Cirrus 1, Stratus 1, Nimbostratus 5, Altostratus 5, Stratocirrus 3, Stratocumulus 2, Altocumulus 7 and Cirrocumulus 1; (a1)–(j1) is an adaptive fractional differential; (a2)–(j2) is of order 0.3; (a3)–(j3) is of order 0.55; (a4)–(j4) is of order 0.7; (a5)–(j5) is of order 0.9

From the direct comparison between Fig. 3 and Fig. 4, it can be seen that the texture extracted by fractional differential G-L definition method is clearer. Compared with the R-L definition method under the same order, the enhancement effect of texture is more obvious, and the extraction effect of texture details is better. Therefore, G-L definition of fractional differential method is suitable for processing images.

In order to quantitatively evaluate the enhancement algorithm proposed in this paper, the information entropy [22] is used to analyze the obtained texture image and objectively evaluate the ability of texture extraction of various methods. The Shannon information entropy of the image represents the amount of information contained in the aggregation feature of the gray distribution in the image. In this paper, the information entropy of each given order is compared which is used as the criterion to extract the integrity of image texture information. For the above ten types of original cloud image samples, the texture images obtained by each differential order with 0.05–0.95 interval of 0.05 are calculated by G-L definition method. The information entropy of texture images corresponding to each order is calculated, and the information entropy of corresponding order is obtained (as shown by the black solid line in Fig. 5). Similarly, for the R-L definition of fractional order differential method, the information entropy of the corresponding order results (shown in the blue solid line in Fig. 5). Comparing the quantitative data curves of G-L definition method and R-L definition method in Fig. 5, it can be found that under the same order the information entropy of most R-L definition method is smaller than that of G-L definition method. This is the same as the previous manual observation, which also shows that the R-L definition method is weaker in texture enhancement. In addition, it can be seen from the graph that the information entropy of the two methods increases with the increase of order, which is not consistent with the results obtained in reference [4].

Experiments show that this is because the image samples in the literature are all artificial textures which have abundant texture information and clear edges. Fractional differential has the best effect on texture-rich image processing. The ground-based cloud image samples belong to natural texture. Some clouds have blurred textures and edges. Therefore, the effect of extracting the texture features of cloud images directly by fractional differential method is not obvious.

It is found that if the cloud image is first enhanced and then extracted by fractional differential, the effect will be greatly improved. Because the fractional differential also enhances the image the fractional differential method are first used to enhance the cloud image. According to the above method, the cloud image is processed by fractional differential, and the information entropy is calculated, the calculation process is shown in Fig. 6. The calculation results are shown in Fig. 7. At this time, it is found that extreme points appear in the curve of information entropy. When the order of fractional differential corresponding to this extreme point is used to process the cloud image, its information entropy is the

largest.

Therefore, the adaptive fractional differential method defined by R-L and the method of dealing with the specified order of the best point are also be compared in this paper, as in Fig. 8. An enhanced cloud images are shown in Figs. 8a0–j0. The results of R-L Adaptive Fractional extraction are shown in Figs. 8a1–j1. The results of best fractional differential extraction with the highest information entropy are shown in Figs. 8a2–j2. From the graph, it can be found that the results of adaptive extraction at this time are close to those of the best order extraction determined manually.

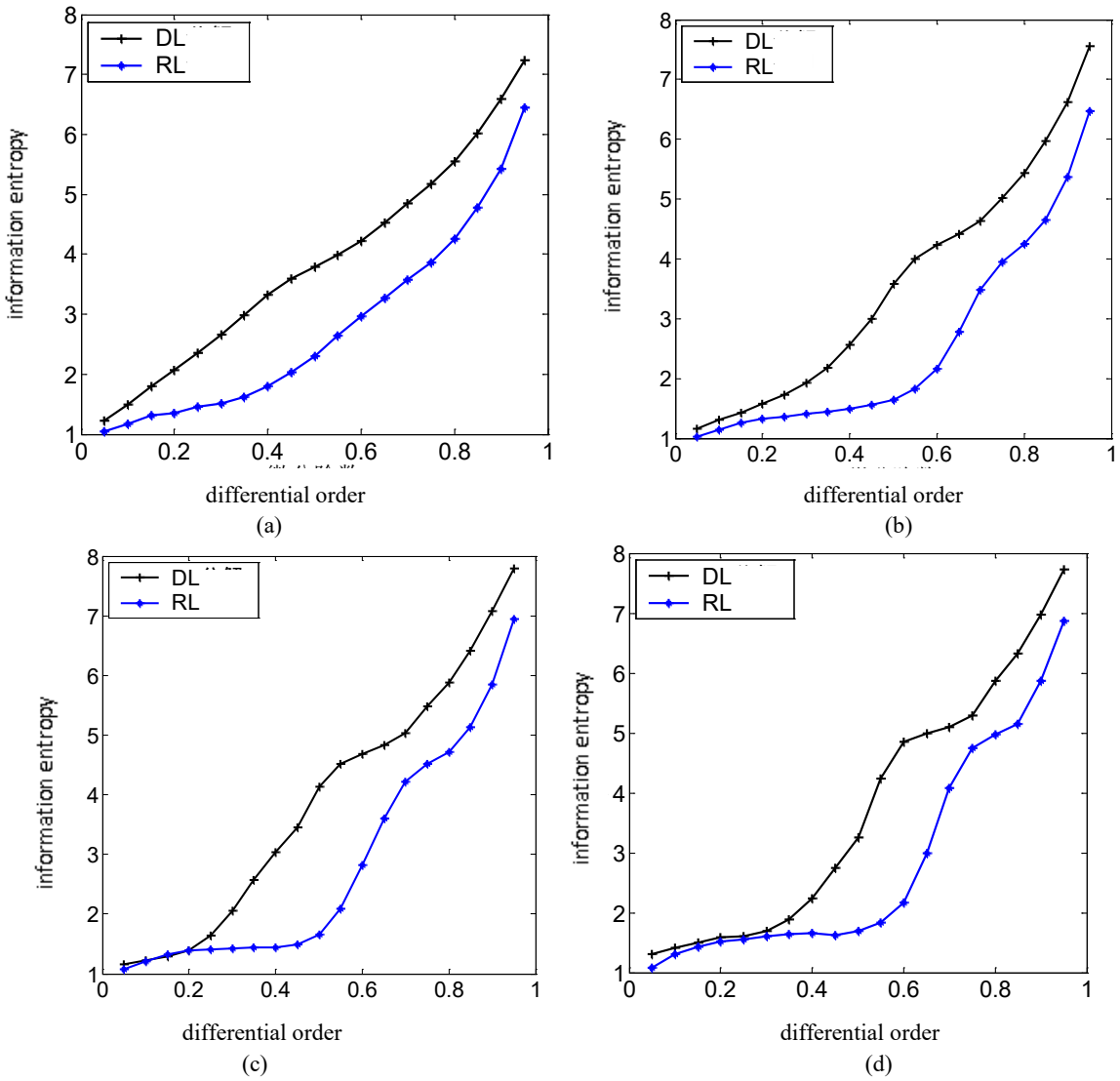

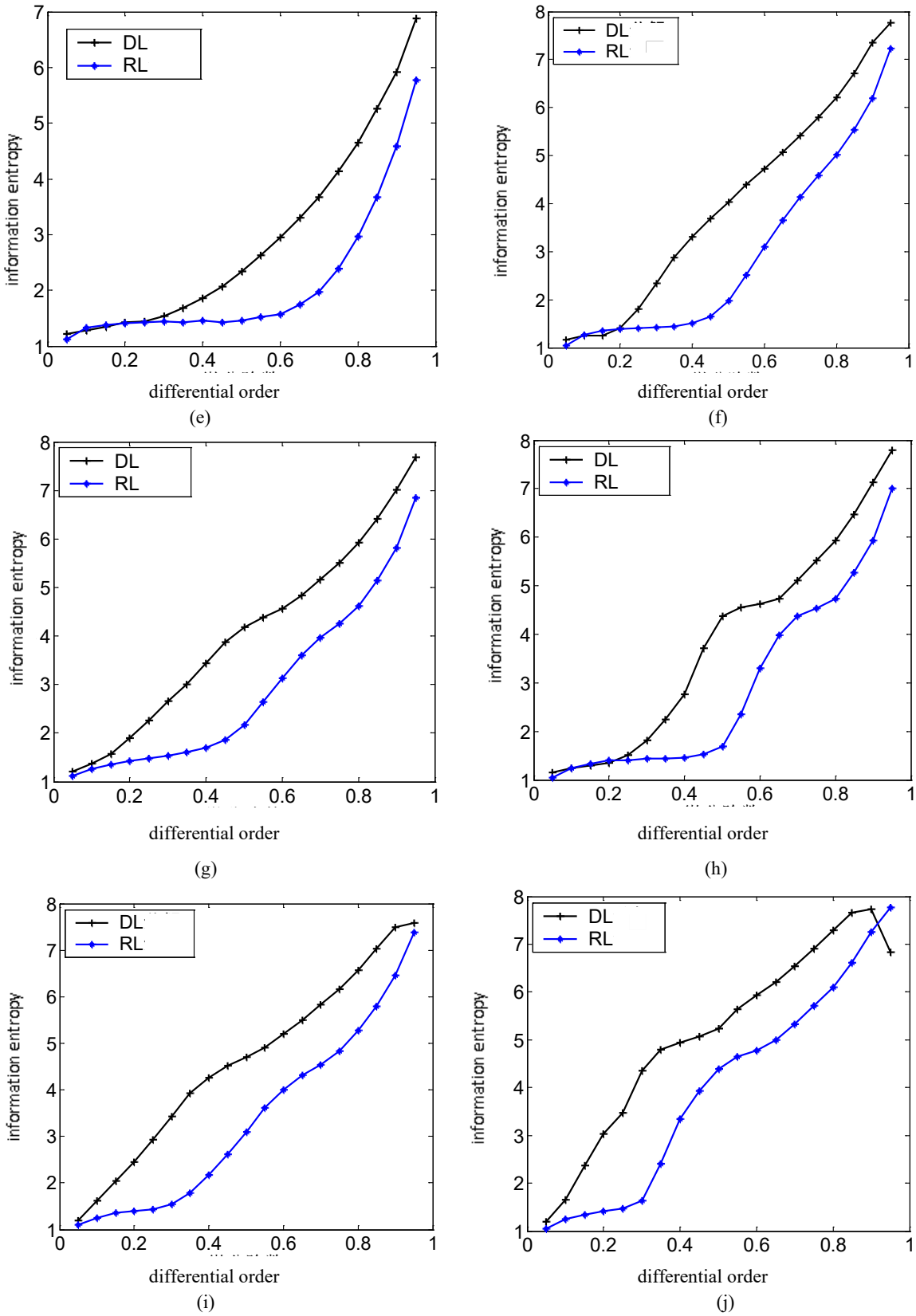

Figure 5: (a)–(j) Information entropy comparison of Fractional Differential Method for selecting order of

Cumulus Humilis 3, Cumulonimbus 1, Cirrus 1, Stratus 1, Nimbostratus 5, Altostratus 5, Stratocirrus 3, Stratocumulus 2, Altocumulus 7 and Cirrocumulus 1

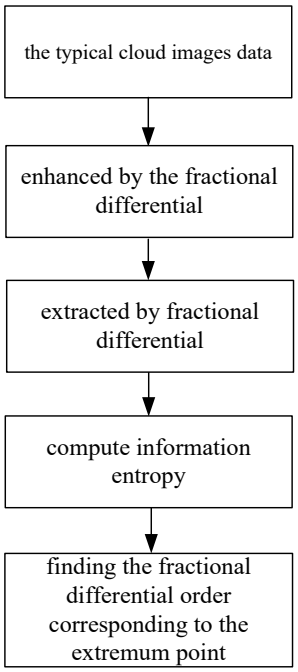

Figure 6: A flow chart illustrating the basic operation of the proposed scheme

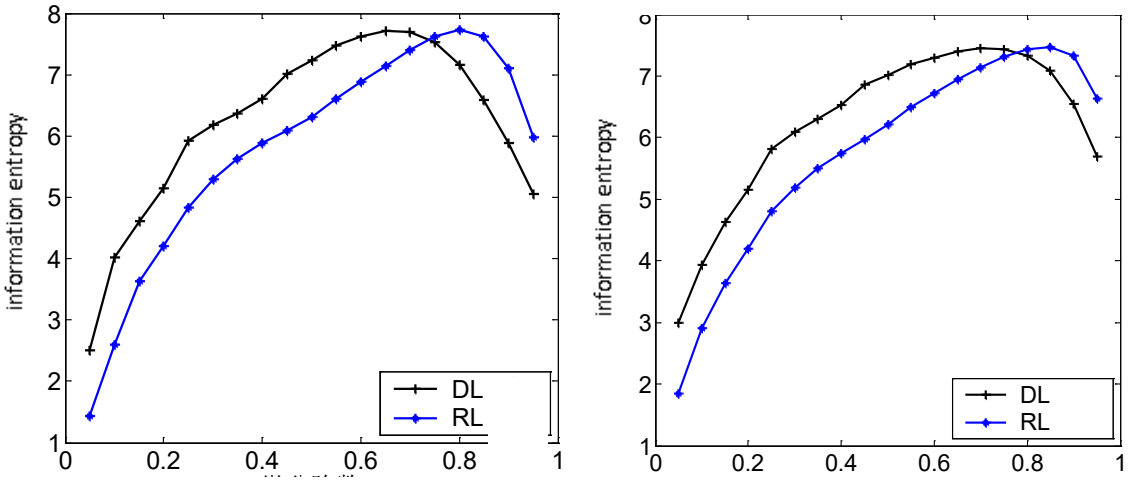

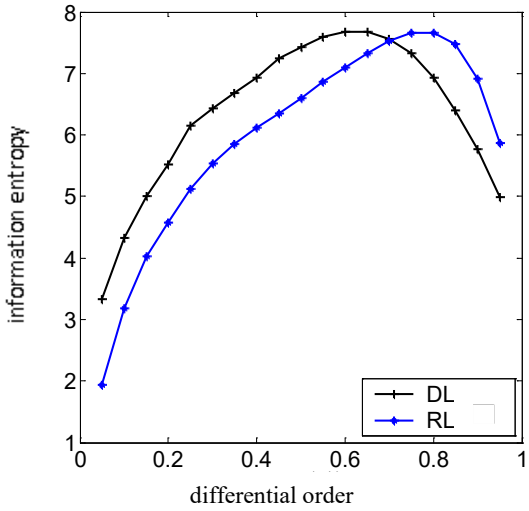
information entropy
differential order
DL
RL

(c)

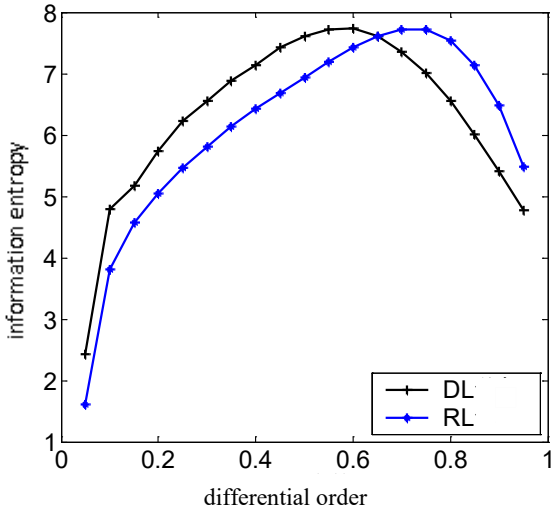
information entropy
differential order
DL
RL

(d)

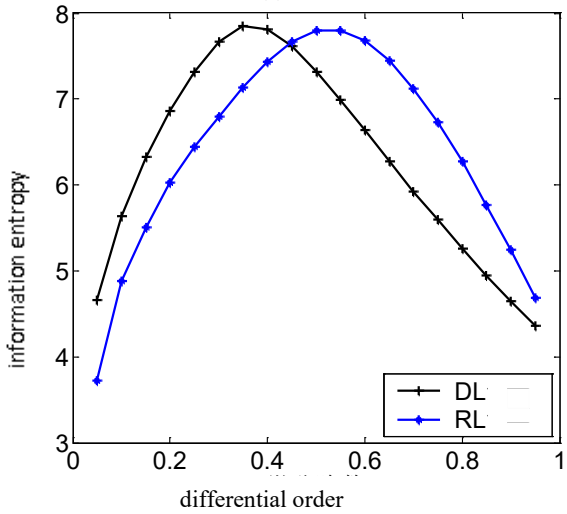
information entropy
differential order
DL
RL

(e)

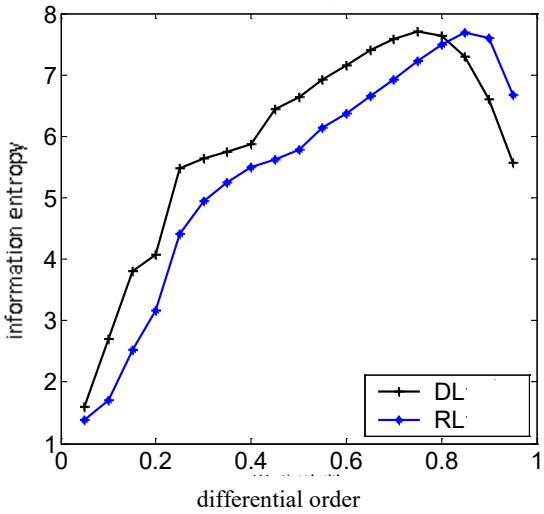
information entropy
differential order
DL
RL

(f)

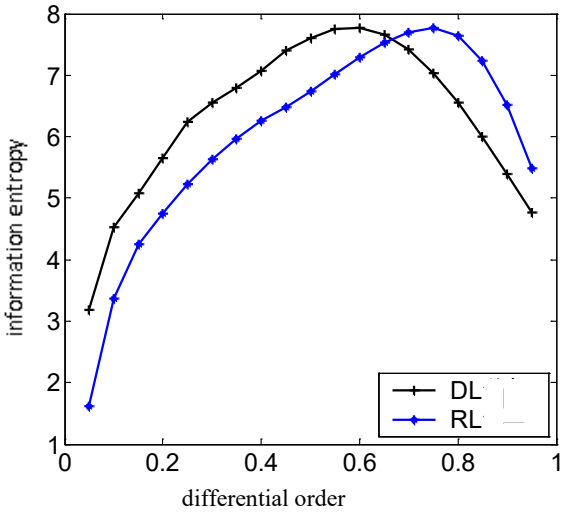
information entropy
differential order
DL
RL

(g)

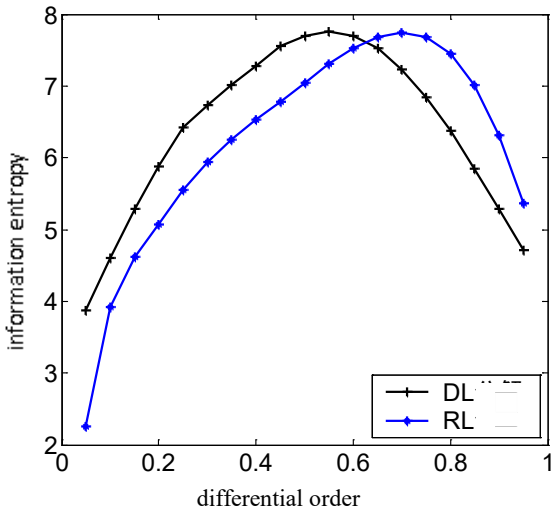
information entropy
differential order
DL
RL

(h)

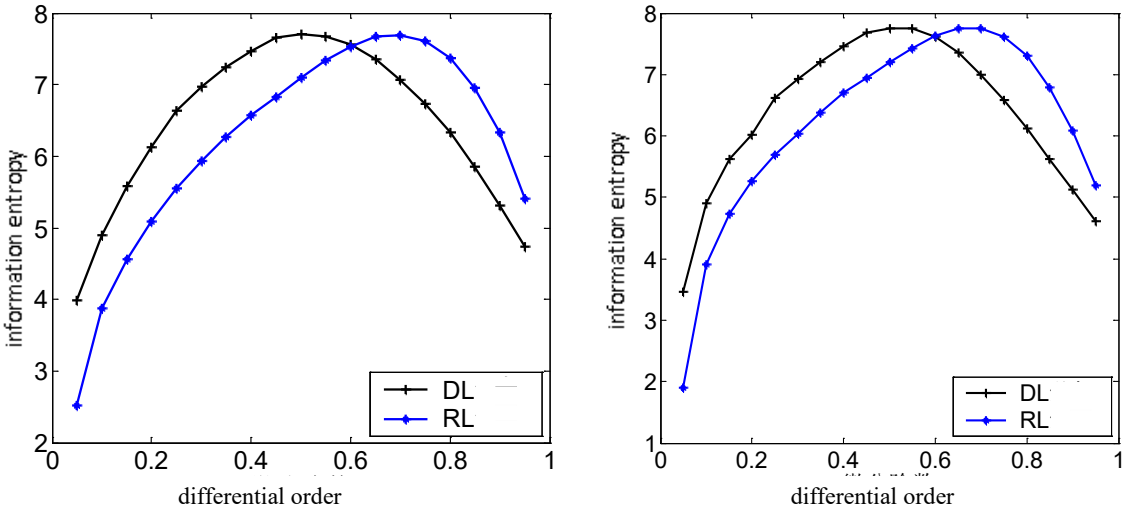

Figure 7: (a)–(j) Information entropy comparison of Fractional Differential Method for selecting order of Cumulus Humilis 3, Cumulonimbus 1, Cirrus 1, Stratus 1, Nimbostratus 5, Altostratus 5, Stratocirrus 3, Stratocumulus 2, Altocumulus 7 and Cirrocumulus 1 after Enhancement

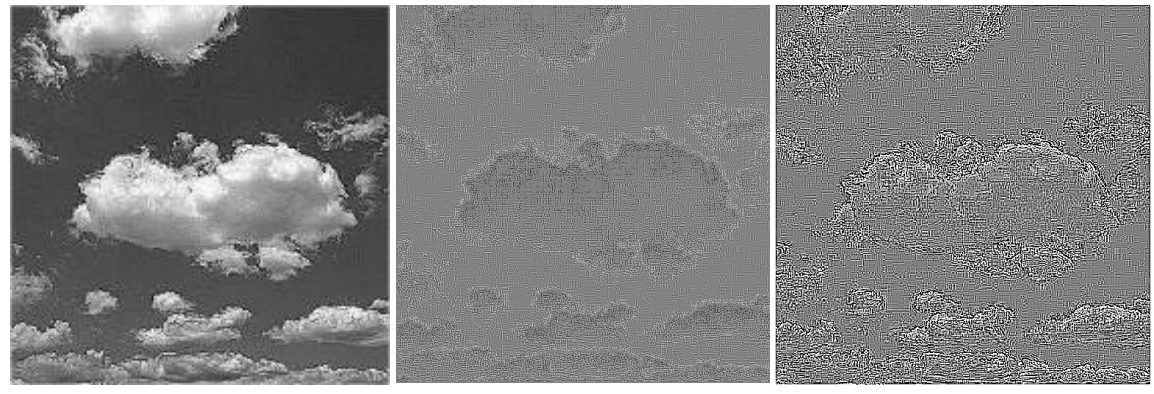

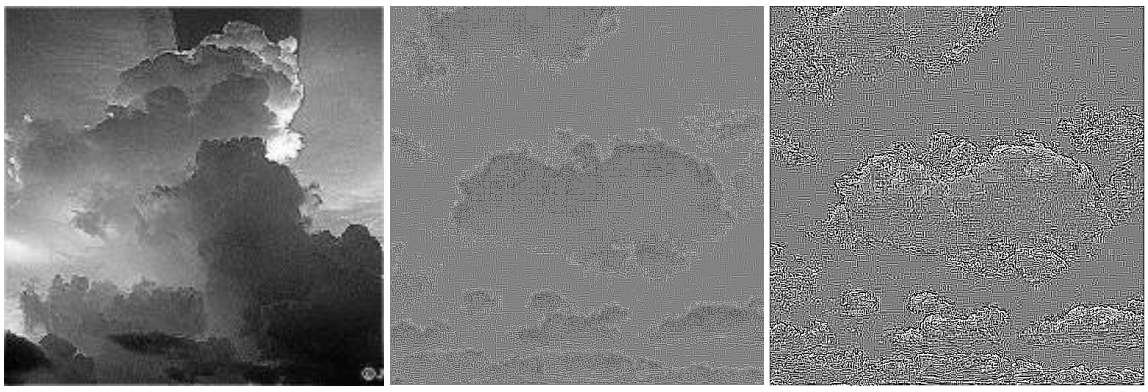

(c0) (c1) (c2)

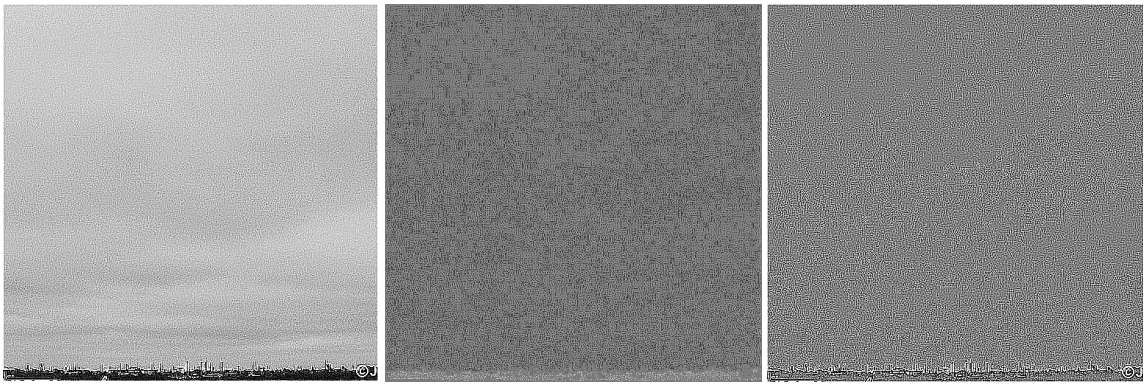

(d0) (d1) (d2)

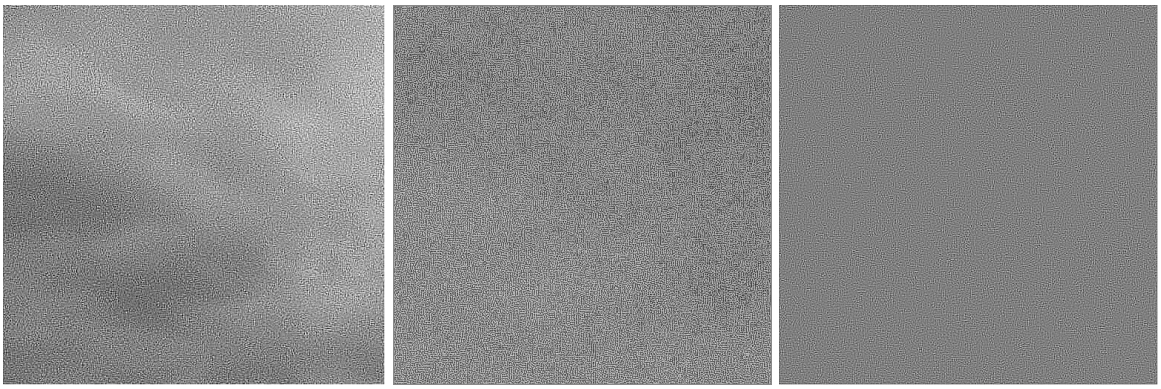

(e0) (e1) (e2)

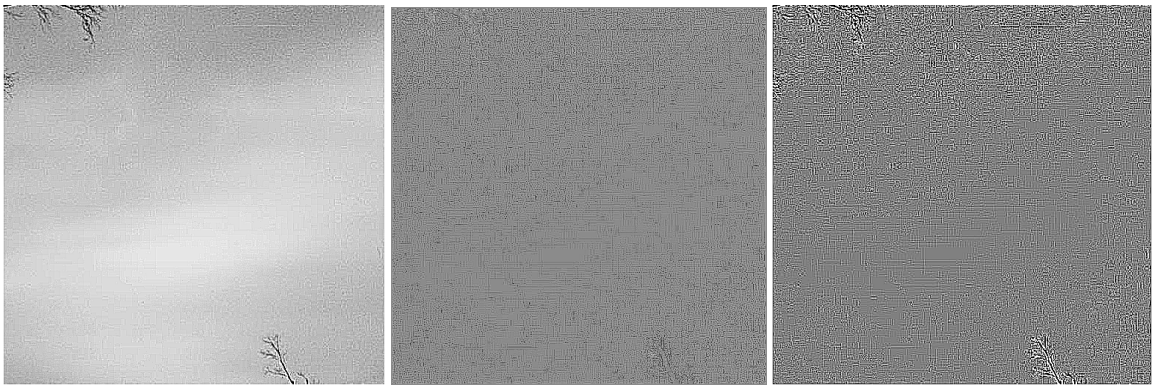

(f0) (f1) (f2)

(g0) (g1) (g2)

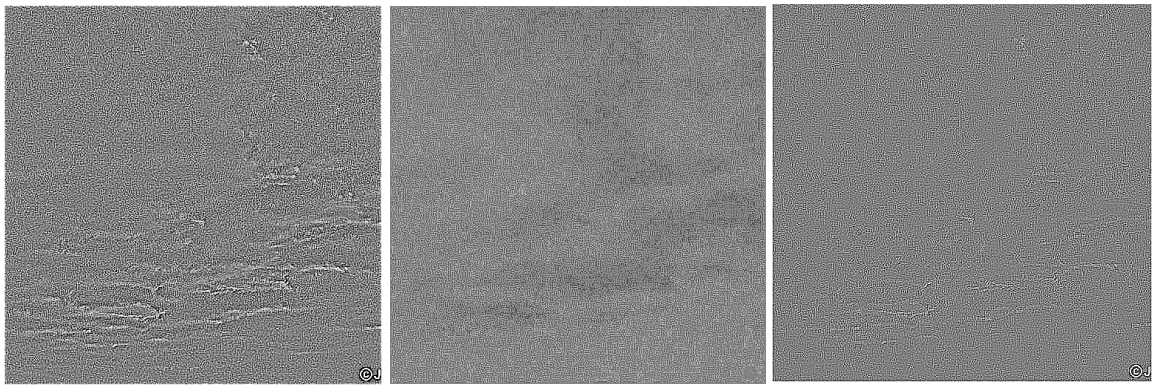

(h0) (h1) (h2)

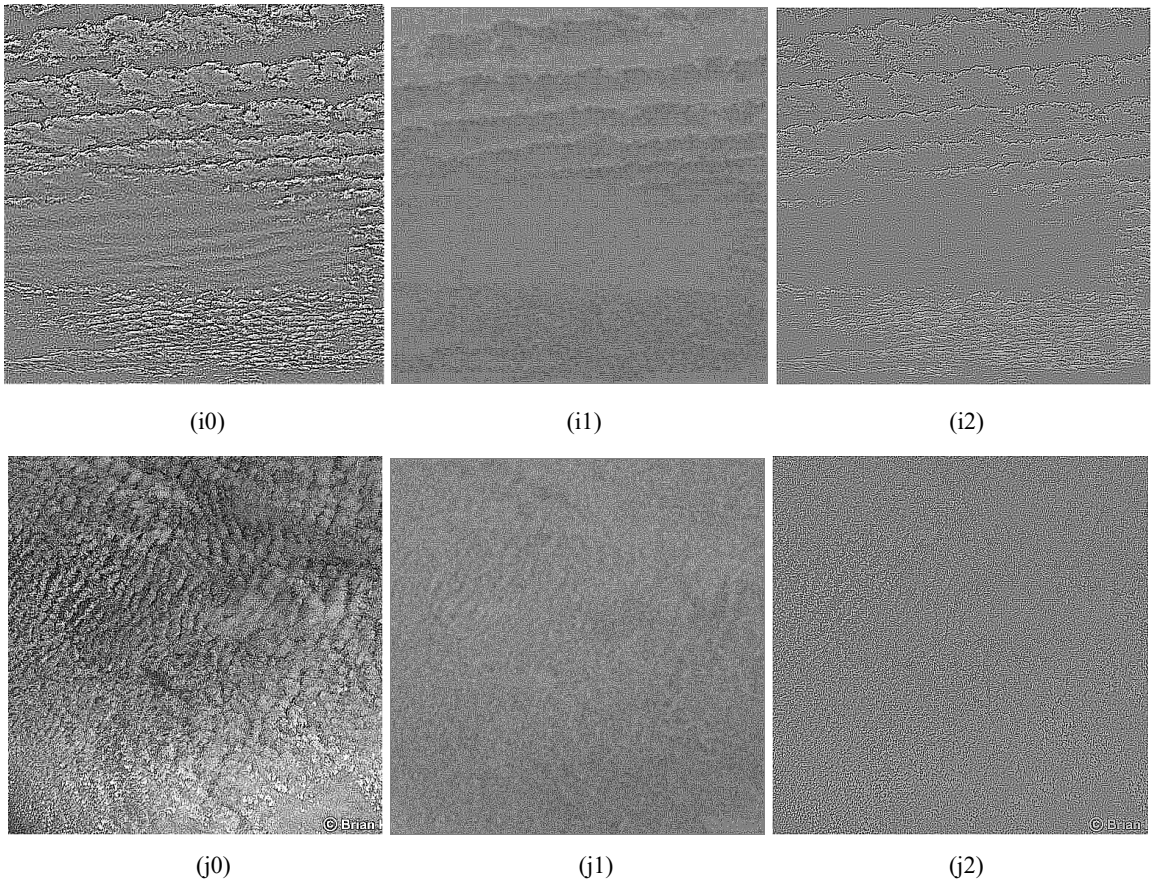

Figure 8: (a0)–(j0) is the image of Cumulus Humilis 3, Cumulonimbus 1, Cirrus 1, Stratus 1, Nimbostratus 5, Altostratus 5, Stratocirrus 3, Stratocumulus 2, Altocumulus 7 and Cirrocumulus 1 enhanced by fractional differential method; (a1)–(j1) is the result of R-L Adaptive Fractional Differential extraction; (a2)–(j2) is the extraction result of fractional differential which has the highest information entropy in the manual R-L extraction result

The above quantitative analysis shows that the improved image enhancement method proposed in this paper by using fractional differential to extract the texture information of ground-based cloud images. The adaptive method can ensure the effect of texture extraction without losing texture details. Quantitative analysis of information entropy shows that the results of self-adaptive determination of order are basically consistent with those of manual determination of optimal order. The computing time and realize the automatic real-time processing of a large number of cloud images can be greatly reduced.

5 Conclusions

In this paper, the pretreatment method of cloud image is studied for reducing the quality of cloud image caused by illumination, rain, haze, dust and other disturbances in order to extract as much effective information as possible from ground-based cloud images and improve the recognition rate of cloud images.

To solve the problem of complex natural texture and difficult to extract from visible ground-based clouds, an adaptive fractional differential enhancement algorithm for ground-based clouds is proposed. The G-L and R-L fractional differential operators are applied to the enhancement of ground-based nephogram. The operator mask based on adaptive differential order is designed and the corresponding mask template is used to process each pixel. After enhancement, the image texture and edge details can be extracted more completely by using adaptive fractional differential algorithm, which simplifies the selection process of differential order. Quantitative analysis of information entropy shows that the results

of self-adaptive determination of order are basically consistent with those of manual determination of optimal order. The computing time and realize the automatic real-time processing of a large number of cloud images can be greatly reduced.

With the development of artificial intelligence technology, cloud image recognition based on in-depth learning technology will surely make great progress to the work of ground-based cloud image recognition in the future [23].

Acknowledgement: This work is supported by the National Natural Science Foundation of China (Grant No. 41775165), Guangxi Key Laboratory of Automatic Detecting Technology and Instruments (YQ21207) and the Qinglan Project of Jiangsu Province.

Funding Statement: The authors received no specific funding for this study.

Conflicts of Interest: The authors declare that they have no conflicts of interest to report regarding the present study.

References

[1] T. C. Gao, L. Liu, S. J. Zhao, X. J. Sun and J. Liu, "The actuality and progress of whole sky cloud sounding techniques," *Journal of Applied Meteorological Science*, vol. 21, no. 1, pp. 101–109, 2010.

[2] X. Y. Chen, A. G. Song, J. Q. Li, X. J. Sun and Y. M. Zhu, "De-illumination method about recognition of ground-based cloud," *Journal of PLA University of Science and Technology (Natural Science Edition)*, vol. 14, no. 5, pp. 578–584, 2013.

[3] M. H. Zhang, H. W. Pan, N. Zhang, X. Q. Xie, Z. Q. Zhang *et al.,* "Cost-sensitive ensemble classification algorithm for medical image," *International Journal of Computational Science and Engineering*, vol. 16, no. 3, pp. 282–288, 2018.

[4] Q. Wang, "Classification and recognition of ground-based cloud based on image features," M.S. thesis, Nanjing University of Information Science & Technology, Nanjing, China, 2013.

[5] T. Y. Zheng and L. Wang, "Using online dictionary learning to improve Bayer pattern image coding," *International Journal of Computational Science and Engineering*, vol. 16, no. 2, pp. 132–140, 2018.

[6] H. Zhang and X. Li, "Enhanced differential evolution with modified parent selection technique for numerical optimisation," *International Journal of Computational Science and Engineering*, vol. 17, no. 1, pp. 98–108, 2018.

[7] W. Wang, "Research on image-based haptic texture display," M.S. thesis, Southeast University, Nanjing, China, 2013.

[8] K. B. Oldham and J. Spanier, *The Fractional Calculus*, Academic Press, New York and London, 1974.

[9] G. Huang, Y. F. Pu, Q. L. Chen and J. L. Zhou, "Application of non-integer step and fractional order differential filter in the image enhancement," *Journal of Sichuan University*, vol. 43, no. 1, pp. 129–136, 2011.

[10] L. M. Zhang and S. B. Zhou, "Feature matching of scale invariant feature transform images based on fractional differential approach," *Journal of Computer Applications*, vol. 31, no. 4, pp. 1019–1023, 2011.

[11] Z. Z. Yang, J. L. Zhou, M. Huang and X. Y. Yan, "Edge detection based on fractional differential," *Journal of Sichuan University*, vol. 40, no. 1, pp. 152–157, 2008.

[12] Z. Z. Yang, J. L. Zhou, Y. X. Yan and M. Huang, "Image enhancement based on fractional differentials," *Journal of Computer-Aided Design & Computer Graphics*, vol. 20, no. 3, pp. 343–348, 2008.

[13] Q. L. Chen, Y. F. Pu, G. Huang and J. L. Zhou, "0～1 order Riemann-Liouville fractional differential enhancing mask of digital image," *Journal of University of Electronic Science and Technology of China*, vol. 40, no. 5, pp. 772–776, 2011.

[14] R. Gou, "Image enhancement based on Riemann-Liouville fractional differential," *Manufacturing Automation*, vol. 35, no. 6, pp. 1–4, 2013.

[15] Y. F. Pu, "Application of fractional differential approach to digital image processing," *Journal of Sichuan University*, vol. 39, no. 3, pp. 124–132, 2007.

[16] Y. F. Pu, J. L. Zhou and X. Yuan, "Fractional differential mask: A fractional differential-based approach for multi-scale texture enhancement," *IEEE Transactions on Image Processing*, vol. 19, no. 2, pp. 491–510, 2010.

[17] Y. F. Pu and W. X. Wang, "Fractional differential masks of digital image and their numerical implementation algorithms," *Acta Automatica Sinica*, vol. 33, no. 11, pp. 1128–1135, 2007.

[18] C. L. Wang, L. B. Lan and S. B. Zhou, "Adaptive fractional differential and its application to image texture enhancement," *Journal of Chongqing University*, vol. 34, no. 2, pp. 32–37, 2011.

[19] S. R. Fountain and T. N. Tan, "Efficient rotation invariant texture features for content-based image retrieval", *Pattern Recognition*, vol. 31, no. 11, pp. 1725–1732, 1998.

[20] H. S. Liu and L. Q. Huang, "A medical image processing method based on human eye visual property," *Opto-Electronic Engineering*, vol. 28, no. 4, pp. 38–41, 2001.

[21] L. B. Lan, "Research on application of fractional differential to digital image processing and support vector machine to face recognition," M.S. thesis, Chongqing University, Chongqing, China, 2011.

[22] M. R. Ubriaco, "Entropies based on fractional calculus," *Physics Letters A*, vol. 373, no. 30, pp. 2516–2519, 2009.

[23] Q. Cui, S. McIntosh and H. Y. Sun, "Identifying materials of photographic images and photorealistic computer generated graphics based on deep CNNs," *Computers, Materials & Continua*, vol. 55, no. 2, pp. 229–241, 2018.